

# Theory of superconductivity in doped cuprates

Shiping Feng and Tianxing Ma

*Department of Physics, Beijing Normal University, Beijing 100875,  
China*

## ABSTRACT

Within the  $t$ - $t'$ - $J$  model, the physical properties of doped cuprates in the superconducting-state are discussed based on the kinetic energy driven superconducting mechanism. We show that the superconducting-state in cuprate superconductors is controlled by both superconducting gap parameter and single particle coherence, and then quantitatively reproduce some main features found in the experiments on cuprate superconductors, including the doping dependence of the superconducting gap parameter and superconducting transition temperature, the electron spectral function at  $[\pi, 0]$  point, the charge asymmetry of superconductivity in the hole and electron doping, and the doping and energy dependence of the incommensurate magnetic scattering at both low and high energies and commensurate  $[\pi, \pi]$  resonance at intermediate energy. We also show that the incommensurate magnetic excitations at high energy have energies greater than the superconducting gap energy, and are present at the superconducting transition temperature.

**Keywords:** Superconductivity; Single particle coherence; Doped cuprates; Incommensurate magnetic scattering; Commensurate resonance

## 1.1 Introduction

Since the discovery of high temperature superconductivity in doped cuprates [1], much effort has concentrated on the superconducting mechanism [2, 3, 4]. After intensive investigations over more than a decade, it has now become clear that the strong electron correlation in doped cuprates plays a crucial role not only for the unusual normal-state behavior but also for the superconducting mechanism [2, 3, 4]. The parent compound of cuprates superconductors is a Mott insulator with the antiferromagnetic long-range order, then changing the carrier concentration by ionic substitution or increasing the oxygen content turns these compounds into the superconducting-state leaving the antiferromagnetic short-range correlation still intact [5]. Moreover, this superconducting-state is dependence of both charge carrier gap function and single particle coherence [6]. As a function of the charge carrier doping concentration, the superconducting transition temperature increases with increasing doping in the underdoped regime, and reaches a maximum in the optimal doping, then decreases in the overdoped regime [7].

In the conventional metals, superconductivity results when electrons pair up into Cooper pairs, which is mediated by the interaction of electrons with phonons [8]. These electron Cooper pairs condense into a coherent macroscopic quantum state that is insensitive to impurities and imperfections in the conventional metals and hence conducts electricity without resistance [8]. As a result, the pairing in the conventional superconductors is always related with an increase in kinetic energy which is overcompensated by the lowering of potential energy [8]. It has been realized that this reduction in the electron potential energy actually corresponds to a decrease in the ionic kinetic energy [9], and thus providing a clear link between the pairing mechanism and phonons. In doped cuprates, the charge carriers form the Cooper pairs when they become superconductors as in the conventional superconductors [10], which is supported by many experimental evidences, including the factor of  $2e$  occurring in the flux quantum and in the Josephson effect, as well as the electrodynamic and thermodynamic properties [10]. Although a possible doping dependent pairing symmetry has been suggested [11], the charge carrier Cooper pairs have a dominated d-wave symmetry around the optimal doping [10, 11]. By virtue of systematic studies using the nuclear magnetic resonance, and muon spin rotation techniques, particularly the inelastic neutron scattering, it has been well established that the antiferromagnetic short-range correlation coexists with the superconducting-state in the whole superconducting regime [12, 13, 14]. Furthermore, the unusual incommensurate magnetic excitations at high energy have energies greater

than the superconducting pairing energy, are present at the superconducting transition temperature, and have spectral weight far exceeding that of the commensurate resonance at intermediate energy [15]. These experimental results provide a clear link between the charge carrier pairing mechanism and magnetic excitations, and also is an indication of the unconventional superconducting mechanism that is responsible for the high superconducting transition temperatures [2]. In this case, it has been argued based on the non-Fermi liquid normal-state that the form of the charge carrier Cooper pairs is determined by the need to reduce the frustrated kinetic energy of charge carriers [3], i.e., the strong frustration of the kinetic energy in the normal-state is partially relieved upon entering the superconducting-state, where the driving attractive force between holes may be attributed to the fact that by sharing a common link two holes minimize the loss of the energy related to breaking antiferromagnetic links, and is therefore mediated by the exchange of spin excitations [16]. Moreover, by solving a model for alkali doped fullerenes within dynamical mean-field theory, it has been argued [17] recently that the strong electron correlation does not suppress superconductivity, but rather seems to favor it because the main ingredient was identified into a pairing mechanism not involving the charge density operator, but other internal degrees of freedom, like the spin, unveiling a kind of the charge-spin separation. The normal-state above the superconducting transition temperature exhibits a number of anomalous properties which is due to the charge-spin separation [2, 3], while the superconducting-state is characterized by the charge-spin recombination. These scenarios are consistent with recent optical experiments [18].

Recently, we [19] have developed a charge-spin separation fermion-spin theory to study the physical properties of doped cuprates, where the electron operator is decoupled as a gauge invariant dressed holon and spin. Within this theoretical framework, we have discussed the unusual normal-state properties of the underdoped cuprates and kinetic energy driven superconducting mechanism, and the results are qualitatively consistent with the experiments. It is shown that the charge transport is mainly governed by the scattering from the dressed holons due to the dressed spin fluctuation, while the scattering from the dressed spins due to the dressed holon fluctuation dominates the spin response [19]. Based on the  $t$ - $J$  model, it is also shown [20] that the dressed holons interact occurring directly through the kinetic energy by exchanging the dressed spin excitations, leading to a net attractive force between the dressed holons. Then the electron Cooper pairs originating from the dressed holon pairing state are due to the charge-spin recombination, and their condensation reveals the superconducting ground-

state, where the maximal superconducting transition temperature occurs around the optimal doping, and then decreases in both underdoped and overdoped regimes [21]. However, the simple  $t$ - $J$  model can not be regarded as a comprehensive model for the quantitative comparison with cuprate superconductors. It has been shown [22] from the angle resolved photoemission spectroscopy experiments that although the highest energy filled electron band is well described by the  $t$ - $J$  model in the direction between the  $[0,0]$  point and the  $[\pi,\pi]$  point (in units of inverse lattice constant) in the momentum space, but both the experimental data near  $[\pi,0]$  point and overall dispersion may be properly accounted by generalizing the  $t$ - $J$  model to include the second- and third-nearest neighbors hopping terms  $t'$  and  $t''$ . Moreover, the additional second neighbor hopping  $t'$  may play an important role in explaining the difference between the electron and hole doping [23]. In this chapter, we discuss the physical properties of cuprate superconductors within the framework of the kinetic energy driven superconducting mechanism. We have performed a systematic study within the  $t$ - $t'$ - $J$  model based on the charge-spin separation fermion-spin theory, and quantitatively reproduced some main features found in the experiments on cuprate superconductors, including the doping dependence of the superconducting gap parameter and superconducting transition temperature [7], the electron spectral function at  $[\pi,0]$  point [22], the charge asymmetry of superconductivity in the hole and electron doping, and the doping and energy dependence of the incommensurate magnetic scattering at both low and high energies [15, 24, 25] and commensurate  $[\pi,\pi]$  resonance at intermediate energy [26, 27]. Our results also show that the effect of the additional second neighbor hopping  $t'$  is to enhance the d-wave superconducting pairing correlation, and suppress the s-wave superconducting pairing correlation.

This chapter is organized as follows. The theory of superconductivity in doped cuprates is presented in Sec. 2. It is shown that the superconducting state in cuprate superconductors is controlled by both superconducting gap function and single particle coherence. In particular, this superconducting state is the conventional Bardeen-Cooper-Schrieffer like, so that some of the basic Bardeen-Cooper-Schrieffer formalism [8] is still valid in discussions of the superconducting transition temperature and electron spectral function, although the pairing mechanism is driven by the kinetic energy by exchanging dressed spin excitations, and other exotic properties are beyond Bardeen-Cooper-Schrieffer theory. In Sec. 3, we calculate explicitly the dynamical spin structure factor of cuprate superconductors in terms of the collective mode in the dressed holon particle-particle channel, and give a quantitative explanation of inelastic neutron scattering experiments on cuprate super-

conductors [15, 26, 27, 24]. In Sec. 4, we discuss the charge asymmetry of superconductivity in hole and electron doping, and show that the maximum achievable superconducting transition temperature in the optimal doping in the electron-doped case is much lower than that of the hole-doped side due to the electron-hole asymmetry. Sec. 5 is devoted to a summary.

## 1.2 Theory of superconductivity

Since the characteristic feature in doped cuprates is the presence of the two-dimensional  $\text{CuO}_2$  plane [5], then it seems evident that the relatively high superconducting transition temperature is closely related to doped  $\text{CuO}_2$  planes. It has been argued that the essential physics of the doped  $\text{CuO}_2$  plane is well described by the  $t$ - $t'$ - $J$  model on a square lattice [2, 22],

$$\begin{aligned}
 H = & -t \sum_{i\hat{\eta}\sigma} C_{i\sigma}^\dagger C_{i+\hat{\eta}\sigma} + t' \sum_{i\hat{\tau}\sigma} C_{i\sigma}^\dagger C_{i+\hat{\tau}\sigma} + \mu \sum_{i\sigma} C_{i\sigma}^\dagger C_{i\sigma} \\
 & + J \sum_{i\hat{\eta}} \mathbf{S}_i \cdot \mathbf{S}_{i+\hat{\eta}}, \tag{1.1}
 \end{aligned}$$

supplemented by the on-site local constraint,

$$\sum_{\sigma} C_{i\sigma}^\dagger C_{i\sigma} \leq 1, \tag{1.2}$$

to avoid the double occupancy, where  $\hat{\eta} = \pm\hat{x}, \pm\hat{y}$ ,  $\hat{\tau} = \pm\hat{x} \pm \hat{y}$ ,  $C_{i\sigma}^\dagger$  ( $C_{i\sigma}$ ) is the electron creation (annihilation) operator,  $\mathbf{S}_i = C_i^\dagger \vec{\sigma} C_i / 2$  is spin operator with  $\vec{\sigma} = (\sigma_x, \sigma_y, \sigma_z)$  as Pauli matrices, and  $\mu$  is the chemical potential. The  $t$ - $J$  type model was originally introduced as an effective Hamiltonian of the large- $U$  Hubbard model [2], where the on-site Coulomb repulsion  $U$  is very large as compared with the electron hopping energy  $t$ , which leads to that electrons become strongly correlated to avoid double occupancy, while the origin of  $t'$  has been discussed theoretically [28], and it appears naturally in mappings from the three-band model for doped cuprates to a one-band  $t$ - $J$  type Hamiltonian. Therefore the strong electron correlation in the  $t$ - $t'$ - $J$  model manifests itself by the electron single occupancy local constraint, which is why the crucial requirement is to impose this electron local constraint for a proper understanding of the physical properties of doped cuprates. To incorporate this local constraint, the charge-spin separation fermion-spin theory [19] has been proposed, where the constrained electron operators are decoupled as,

$$C_{i\uparrow} = h_{i\uparrow}^\dagger S_i^-, \quad C_{i\downarrow} = h_{i\downarrow}^\dagger S_i^+, \tag{1.3}$$

where the spinful fermion operator  $h_{i\sigma} = e^{-i\Phi_{i\sigma}} h_i$  describes the charge degree of freedom together with some effects of the spin configuration rearrangements due to the presence of the doped hole itself (dressed holon), while the spin operator  $S_i$  describes the spin degree of freedom (dressed spin), then the electron on-site local constraint for the single occupancy,

$$\begin{aligned} \sum_{\sigma} C_{i\sigma}^{\dagger} C_{i\sigma} &= S_i^+ h_{i\uparrow} h_{i\uparrow}^{\dagger} S_i^- + S_i^- h_{i\downarrow} h_{i\downarrow}^{\dagger} S_i^+ \\ &= h_i h_i^{\dagger} (S_i^+ S_i^- + S_i^- S_i^+) = 1 - h_i^{\dagger} h_i \leq 1, \end{aligned} \quad (1.4)$$

is satisfied in analytical calculations, and the double spinful fermion occupancy,

$$h_{i\sigma}^{\dagger} h_{i-\sigma}^{\dagger} = e^{i\Phi_{i\sigma}} h_i^{\dagger} h_i^{\dagger} e^{i\Phi_{i-\sigma}} = 0, \quad h_{i\sigma} h_{i-\sigma} = e^{-i\Phi_{i\sigma}} h_i h_i e^{-i\Phi_{i-\sigma}} = 0, \quad (1.5)$$

are ruled out automatically. It has been shown that these dressed holon and spin are gauge invariant [19], and in this sense, they are real [4]. At the half-filling, the  $t$ - $t'$ - $J$  model is reduced to the antiferromagnetic Heisenberg model, where there is no charge degree of freedom, and then the real spin excitation is described by the spin operator  $S_i$ . Since the phase factor  $\Phi_{i\sigma}$  is separated from the bare spinon operator, and then it describes a spin cloud [19, 29]. Therefore the dressed holon  $h_{i\sigma}$  is a spinless fermion  $h_i$  (bare holon) incorporated the spin cloud  $e^{-i\Phi_{i\sigma}}$  (magnetic flux), thus is a magnetic dressing. In other words, the gauge invariant dressed holon carries some spin messages, i.e., it shares its nontrivial spin environment [29]. Although in common sense  $h_{i\sigma}$  is not a real spinful fermion, it behaves like a spinful fermion. The spirit of the charge-spin separation fermion-spin theory is that the electron operator can be mapped as a product of the spin operator and spinful fermion operator, this is very similar to the case of the bosonization in one-dimensional interacting electron systems, where the electron operators are mapped onto the boson (electron density) representation, and then the recast Hamiltonian is exactly solvable. In this charge-spin separation fermion-spin representation, the low-energy behavior of the  $t$ - $t'$ - $J$  model (1) can be expressed as [19],

$$\begin{aligned} H &= -t \sum_{i\hat{\eta}} (h_{i\uparrow} S_i^+ h_{i+\hat{\eta}\uparrow}^{\dagger} S_{i+\hat{\eta}}^- + h_{i\downarrow} S_i^- h_{i+\hat{\eta}\downarrow}^{\dagger} S_{i+\hat{\eta}}^+) \\ &+ t' \sum_{i\hat{\tau}} (h_{i\uparrow} S_i^+ h_{i+\hat{\tau}\uparrow}^{\dagger} S_{i+\hat{\tau}}^- + h_{i\downarrow} S_i^- h_{i+\hat{\tau}\downarrow}^{\dagger} S_{i+\hat{\tau}}^+) \\ &- \mu \sum_{i\sigma} h_{i\sigma}^{\dagger} h_{i\sigma} + J_{\text{eff}} \sum_{i\hat{\eta}} \mathbf{S}_i \cdot \mathbf{S}_{i+\hat{\eta}}, \end{aligned} \quad (1.6)$$

with  $J_{\text{eff}} = (1 - x)^2 J$ , and  $x = \langle h_{i\sigma}^\dagger h_{i\sigma} \rangle = \langle h_i^\dagger h_i \rangle$  is the hole doping concentration. As a consequence, the kinetic energy terms in the  $t$ - $t'$ - $J$  model have been expressed as the dressed holon-spin interactions, which dominate the essential physics of doped cuprates, while the magnetic energy term is only to form an adequate dressed spin configuration [3]. This reflects that even the kinetic energy terms in the  $t$ - $t'$ - $J$  Hamiltonian have strong Coulombic contributions due to the restriction of no doubly occupancy of a given site. This is why the interaction between the dressed holons (dressed spins) can occur directly through the kinetic energy by exchanging dressed spin (dressed holon) excitations [19, 20].

It has been shown that the superconducting state in cuprate superconductors is characterized by the electron Cooper pairs, forming superconducting quasiparticles [10]. Moreover, the angle resolved photoemission spectroscopy measurements [30] show that in the real space the gap function and pairing force have a range of one lattice spacing. These indicate that the order parameter for the electron Cooper pair can be expressed as,

$$\Delta = \langle C_{i\uparrow}^\dagger C_{i+\hat{\eta}\downarrow}^\dagger - C_{i\downarrow}^\dagger C_{i+\hat{\eta}\uparrow}^\dagger \rangle = \langle h_{i\uparrow} h_{i+\hat{\eta}\downarrow} S_i^+ S_{i+\hat{\eta}}^- - h_{i\downarrow} h_{i+\hat{\eta}\uparrow} S_i^- S_{i+\hat{\eta}}^+ \rangle. \quad (1.7)$$

In the doped regime without the antiferromagnetic long-range order, the dressed spins form a disordered spin liquid state, where the dressed spin correlation function  $\langle S_i^+ S_{i+\hat{\eta}}^- \rangle = \langle S_i^- S_{i+\hat{\eta}}^+ \rangle$ , then the order parameter for the electron Cooper pair in Eq. (7) can be written as,

$$\Delta = -\langle S_i^+ S_{i+\hat{\eta}}^- \rangle \Delta_h, \quad (1.8)$$

with the dressed holon pairing order parameter,

$$\Delta_h = \langle h_{i+\hat{\eta}\downarrow} h_{i\uparrow} - h_{i+\hat{\eta}\uparrow} h_{i\downarrow} \rangle, \quad (1.9)$$

which shows that the superconducting order parameter is related to the dressed holon pairing amplitude, and is proportional to the number of doped holes, and not to the number of electrons. However, in the extreme low doped regime with the antiferromagnetic long-range order, where the dressed spin correlation function  $\langle S_i^+ S_{i+\hat{\eta}}^- \rangle \neq \langle S_i^- S_{i+\hat{\eta}}^+ \rangle$ , then the conduct is disrupted by the antiferromagnetic long-range order, and therefore there is no mixing of superconductivity and the antiferromagnetic long-range order [31]. In the case without the antiferromagnetic long-range order, we [20, 21] have discussed the kinetic energy driven superconductivity within the  $t$ - $J$  model, and some qualitative results are obtained. Following our previous discussions, we study this issue within the  $t$ - $t'$ - $J$  model for a quantitative understanding of the physical properties of cuprates superconductors.

The quantum spin operators obey the Pauli spin algebra, i.e., the spin one-half raising and lowering operators  $S_i^+$  and  $S_i^-$  behave as fermions on the same site and as bosons on different sites, and therefore this problem can be discussed in terms of the two-time spin Green's function within the Tyablikov scheme [32]. In the present case, we define the dressed holon diagonal and off-diagonal Green's functions as,

$$g(i-j, t-t') = -i\theta(t-t')\langle\{h_{i\sigma}(t), h_{j\sigma}^\dagger(t')\}\rangle = \langle\langle h_{i\sigma}(t); h_{j\sigma}^\dagger(t') \rangle\rangle, \quad (1.10)$$

$$\mathfrak{S}(i-j, t-t') = -i\theta(t-t')\langle\{h_{i\downarrow}(t), h_{j\uparrow}(t')\}\rangle = \langle\langle h_{i\downarrow}(t); h_{j\uparrow}(t') \rangle\rangle, \quad (1.11)$$

$$\mathfrak{S}^\dagger(i-j, t-t') = -i\theta(t-t')\langle\{h_{i\uparrow}^\dagger(t), h_{j\downarrow}^\dagger(t')\}\rangle = \langle\langle h_{i\uparrow}^\dagger(t); h_{j\downarrow}^\dagger(t') \rangle\rangle, \quad (1.12)$$

and the dressed spin Green's functions as,

$$D(i-j, t-t') = -i\theta(t-t')\langle[S_i^+(t), S_j^-(t')]\rangle = \langle\langle S_i^+(t); S_j^-(t') \rangle\rangle, \quad (1.13)$$

$$D_z(i-j, t-t') = -i\theta(t-t')\langle[S_i^z(t), S_j^z(t')]\rangle = \langle\langle S_i^z(t); S_j^z(t') \rangle\rangle, \quad (1.14)$$

respectively, where  $\langle \dots \rangle$  is an average over the ensemble. Within the mean-field approximation, the  $t$ - $t'$ - $J$  model can be decoupled as,

$$H_{\text{MFA}} = H_t + H_J + H_0, \quad (1.15)$$

$$H_t = \chi_1 t \sum_{i\hat{\eta}\sigma} h_{i+\hat{\eta}\sigma}^\dagger h_{i\sigma} - \chi_2 t' \sum_{i\hat{\tau}\sigma} h_{i+\hat{\tau}\sigma}^\dagger h_{i\sigma} - \mu \sum_{i\sigma} h_{i\sigma}^\dagger h_{i\sigma}, \quad (1.16)$$

$$\begin{aligned} H_J &= \frac{1}{2} J_{\text{eff}} \epsilon \sum_{i\hat{\eta}} (S_i^+ S_{i+\hat{\eta}}^- + S_i^- S_{i+\hat{\eta}}^+) + J_{\text{eff}} \sum_{i\hat{\eta}} S_i^z S_{i+\hat{\eta}}^z \\ &\quad - t' \phi_2 \sum_{i\hat{\tau}} (S_i^+ S_{i+\hat{\tau}}^- + S_i^- S_{i+\hat{\tau}}^+), \end{aligned} \quad (1.17)$$

$$H_0 = -2N Z t \phi_1 \chi_1 + 2N Z t' \phi_2 \chi_2, \quad (1.18)$$

with  $\epsilon = 1 + 2t\phi_1/J_{\text{eff}}$ ,  $Z$  is the number of the nearest neighbor or second-nearest neighbor sites,  $N$  is the number of sites, the dressed holon's particle-hole parameters  $\phi_1 = \langle h_{i\sigma}^\dagger h_{i+\hat{\eta}\sigma} \rangle$  and  $\phi_2 = \langle h_{i\sigma}^\dagger h_{i+\hat{\tau}\sigma} \rangle$ , and the spin correlation functions  $\chi_1 = \langle S_i^+ S_{i+\hat{\eta}}^- \rangle$  and  $\chi_2 = \langle S_i^+ S_{i+\hat{\tau}}^- \rangle$ . Therefore in the mean-field level, the dressed spin system is an anisotropic away from the half-filling [33], and we have defined the two dressed spin Green's function  $D(i-j, t-t')$  in Eq. (13) and  $D_z(i-j, t-t')$  in Eq. (14) to describe the dressed spin propagations. In the doped regime without the antiferromagnetic long-range order, i.e.,  $\langle S_i^z \rangle = 0$ , a mean-field theory of the  $t$ - $J$  model based on the fermion-spin theory has been developed [33] within the Kondo-Yamaji decoupling scheme [34], which is a stage one-step further than the



Tyablikov's decoupling scheme. Following their discussions [33], we can obtain the mean-field dressed holon and spin Green's functions of the  $t$ - $t'$ - $J$  model as,

$$g^{(0)}(k) = \frac{1}{i\omega_n - \xi_{\mathbf{k}}}, \quad (1.19)$$

$$D^{(0)}(p) = \frac{B_{\mathbf{p}}}{2\omega_{\mathbf{p}}} \left( \frac{1}{ip_m - \omega_{\mathbf{p}}} - \frac{1}{ip_m + \omega_{\mathbf{p}}} \right), \quad (1.20)$$

$$D_z^{(0)}(p) = \frac{B_z(\mathbf{p})}{2\omega_z(\mathbf{p})} \left( \frac{1}{ip_m - \omega_z(\mathbf{p})} - \frac{1}{ip_m + \omega_z(\mathbf{p})} \right), \quad (1.21)$$

respectively, where the four-vector notation  $k = (\mathbf{k}, i\omega_n)$ ,  $p = (\mathbf{p}, ip_m)$ ,  $B_{\mathbf{p}} = 2\lambda_1(A_1\gamma_{\mathbf{p}} - A_2) - \lambda_2(2\chi_2^z\gamma'_{\mathbf{p}} - \chi_2)$ ,  $B_z(\mathbf{p}) = \epsilon\chi_1\lambda_1(\gamma_{\mathbf{p}} - 1) - \chi_2\lambda_2(\gamma'_{\mathbf{p}} - 1)$ ,  $\lambda_1 = 2ZJ_{eff}$ ,  $\lambda_2 = 4Z\phi_2t'$ ,  $\gamma_{\mathbf{k}} = (1/Z)\sum_{\hat{\eta}} e^{i\mathbf{k}\cdot\hat{\eta}}$ ,  $\gamma'_{\mathbf{k}} = (1/Z)\sum_{\hat{\tau}} e^{i\mathbf{k}\cdot\hat{\tau}}$ ,  $A_1 = \epsilon\chi_1^z + \chi_1/2$ ,  $A_2 = \chi_1^z + \epsilon\chi_1/2$ , the spin correlation functions  $\chi_1^z = \langle S_i^z S_{i+\hat{\eta}}^z \rangle$  and  $\chi_2^z = \langle S_i^z S_{i+\hat{\tau}}^z \rangle$ , and the mean-field dressed holon and spin excitation spectra are given by,

$$\xi_{\mathbf{k}} = Zt\chi_1\gamma_{\mathbf{k}} - Zt'\chi_2\gamma'_{\mathbf{k}} - \mu, \quad (1.22)$$

$$\begin{aligned} \omega_{\mathbf{p}}^2 &= \lambda_1^2 \left[ (A_4 - \alpha\epsilon\chi_1^z\gamma_{\mathbf{p}} - \frac{1}{2Z}\alpha\epsilon\chi_1)(1 - \epsilon\gamma_{\mathbf{p}}) \right. \\ &\quad + \frac{1}{2}\epsilon(A_3 - \frac{1}{2}\alpha\chi_1^z - \alpha\chi_1\gamma_{\mathbf{p}})(\epsilon - \gamma_{\mathbf{p}}) \\ &\quad + \lambda_2^2[\alpha(\chi_2^z\gamma'_{\mathbf{p}} - \frac{3}{2Z}\chi_2)\gamma'_{\mathbf{p}} + \frac{1}{2}(A_5 - \frac{1}{2}\alpha\chi_2^z)] \\ &\quad + \lambda_1\lambda_2[\alpha\chi_1^z(1 - \epsilon\gamma_{\mathbf{p}})\gamma'_{\mathbf{p}} + \frac{1}{2}\alpha(\chi_1\gamma'_{\mathbf{p}} - C_3)(\epsilon - \gamma_{\mathbf{p}}) \\ &\quad \left. + \alpha\gamma'_{\mathbf{p}}(C_3^z - \epsilon\chi_2^z\gamma_{\mathbf{p}}) - \frac{1}{2}\alpha\epsilon(C_3 - \chi_2\gamma_{\mathbf{p}}) \right], \end{aligned} \quad (1.23)$$

$$\begin{aligned} \omega_z^2(\mathbf{p}) &= \epsilon\lambda_1^2(\epsilon A_3 - \frac{1}{Z}\alpha\chi_1 - \alpha\chi_1\gamma_{\mathbf{p}})(1 - \gamma_{\mathbf{p}}) + \lambda_2^2 A_5(1 - \gamma'_{\mathbf{p}}) \\ &\quad + \lambda_1\lambda_2[\alpha\epsilon C_3(\gamma_{\mathbf{p}} + \gamma'_{\mathbf{p}} - 2) + \alpha\chi_2\gamma_{\mathbf{p}}(1 - \gamma'_{\mathbf{p}})], \end{aligned} \quad (1.24)$$

with  $A_3 = \alpha C_1 + (1 - \alpha)/(2Z)$ ,  $A_4 = \alpha C_1^z + (1 - \alpha)/(4Z)$ ,  $A_5 = \alpha C_2 + (1 - \alpha)/(2Z)$ , and the spin correlation functions  $C_1 = (1/Z^2)\sum_{\hat{\eta},\hat{\eta}'} \langle S_{i+\hat{\eta}}^+ S_{i+\hat{\eta}'}^- \rangle$ ,  $C_1^z = (1/Z^2)\sum_{\hat{\eta},\hat{\eta}'} \langle S_{i+\hat{\eta}}^z S_{i+\hat{\eta}'}^z \rangle$ ,  $C_2 = (1/Z^2)\sum_{\hat{\tau},\hat{\tau}'} \langle S_{i+\hat{\tau}}^+ S_{i+\hat{\tau}'}^- \rangle$ , and  $C_3 = (1/Z)\sum_{\hat{\tau}} \langle S_{i+\hat{\tau}}^+ S_{i+\hat{\tau}}^- \rangle$ ,  $C_3^z = (1/Z)\sum_{\hat{\tau}} \langle S_{i+\hat{\tau}}^z S_{i+\hat{\tau}}^z \rangle$ . In order to satisfy the sum rule of the correlation function  $\langle S_i^+ S_i^- \rangle = 1/2$  in the case without the antiferromagnetic long-range order, the important decoupling parameter  $\alpha$  has been introduced in the mean-field calculation [33, 34], which can be regarded as the vertex correction.

We [20, 21] have shown that the dressed holon-spin coupling occurring in the kinetic energy terms in the  $t$ - $t'$ - $J$  model (6) is quite strong. These interactions (kinetic energy terms) can induce the dressed holon pairing state (then the electron pairing state and superconductivity) by exchanging dressed spin excitations in the higher power of the hole doping concentration  $x$ . For discussion of superconductivity caused by the strong dressed holon-spin interactions, we follow the Eliashberg's strong coupling theory [35], and obtain the self-consistent equations in terms of the equation of motion method [36, 19] that satisfied by the full dressed holon diagonal and off-diagonal Green's functions as,

$$g(k) = g^{(0)}(k) + g^{(0)}(k)[\Sigma_1^{(h)}(k)g(k) - \Sigma_2^{(h)}(-k)\mathfrak{S}^\dagger(k)], \quad (1.25)$$

$$\mathfrak{S}^\dagger(k) = g^{(0)}(-k)[\Sigma_1^{(h)}(-k)\mathfrak{S}^\dagger(-k) + \Sigma_2^{(h)}(-k)g(k)], \quad (1.26)$$

respectively, where the dressed holon self-energies are obtained from the dressed spin bubble as [19, 20],

$$\begin{aligned} \Sigma_1^{(h)}(k) &= \frac{1}{N^2} \sum_{\mathbf{p}, \mathbf{p}'} (Zt\gamma_{\mathbf{p}+\mathbf{p}'+\mathbf{k}} - Zt'\gamma'_{\mathbf{p}+\mathbf{p}'+\mathbf{k}})^2 \frac{1}{\beta} \sum_{ip_m} g(p+k) \\ &\times \frac{1}{\beta} \sum_{ip'_m} D^{(0)}(p')D^{(0)}(p'+p), \end{aligned} \quad (1.27)$$

$$\begin{aligned} \Sigma_2^{(h)}(k) &= \frac{1}{N^2} \sum_{\mathbf{p}, \mathbf{p}'} (Zt\gamma_{\mathbf{p}+\mathbf{p}'+\mathbf{k}} - Zt'\gamma'_{\mathbf{p}+\mathbf{p}'+\mathbf{k}})^2 \frac{1}{\beta} \sum_{ip_m} \mathfrak{S}(-p-k) \\ &\times \frac{1}{\beta} \sum_{ip'_m} D^{(0)}(p')D^{(0)}(p'+p). \end{aligned} \quad (1.28)$$

In the above calculations of the dressed holon self-energies, the dressed spin part has been limited to the mean-field level, i.e., the full dressed spin Green's function  $D(p)$  in Eqs. (27) and (28) has been replaced as the mean-field dressed spin Green's function (20), since the theoretical results of the normal-state charge transport obtained at this level are consistent with the experimental data [19, 37].

In the self-consistent equations (25) and (26), the self-energy function  $\Sigma_2^{(h)}(k)$  describes the effective dressed holon gap function, since both doping and temperature dependence of the pairing force and dressed holon gap function have been incorporated into  $\Sigma_2^{(h)}(k)$ . Furthermore, the self-energy function  $\Sigma_1^{(h)}(k)$  renormalizes the mean-field dressed holon spectrum, and therefore it describes the single particle (quasiparticle) coherence. Moreover,

the self-energy function  $\Sigma_2^{(h)}(k)$  is an even function of  $i\omega_n$ , while the other self-energy function  $\Sigma_1^{(h)}(k)$  is not. For the convenience, the self-energy function  $\Sigma_1^{(h)}(k)$  can be broken up into its symmetric and antisymmetric parts as,  $\Sigma_1^{(h)}(k) = \Sigma_{1e}^{(h)}(k) + i\omega_n \Sigma_{1o}^{(h)}(k)$ , then both  $\Sigma_{1e}^{(h)}(k)$  and  $\Sigma_{1o}^{(h)}(k)$  are even functions of  $i\omega_n$ . In this case, the charge carrier single particle (quasiparticle) coherent weight can be defined as  $Z_F^{-1}(k) = 1 - \Sigma_{1o}^{(h)}(k)$ , then the dressed holon diagonal and off-diagonal Green's functions in Eqs. (25) and (26) can be rewritten as,

$$g(k) = \frac{i\omega_n Z_F^{-1}(k) + \xi_{\mathbf{k}} + \Sigma_{1e}^{(h)}(k)}{[i\omega_n Z_F^{-1}(k)]^2 - [\xi_{\mathbf{k}} + \Sigma_{1e}^{(h)}(k)]^2 - [\Sigma_2^{(h)}(k)]^2}, \quad (1.29)$$

$$\mathfrak{S}^\dagger(k) = -\frac{\Sigma_2^{(h)}(k)}{[i\omega_n Z_F^{-1}(k)]^2 - [\xi_{\mathbf{k}} + \Sigma_{1e}^{(h)}(k)]^2 - [\Sigma_2^{(h)}(k)]^2}. \quad (1.30)$$

As in the conventional superconductor [35], the retarded function  $\text{Re}\Sigma_{1e}^{(h)}(k)$  is a constant, independent of  $(\mathbf{k}, \omega)$ , and therefore it just renormalizes the chemical potential. In this case, it can be dropped. Furthermore, we only study the static limit of the effective dressed holon gap function and single particle coherent weight, i.e.,  $\Sigma_2^{(h)}(k) = \bar{\Delta}_h(\mathbf{k})$ , and  $Z_F^{-1}(\mathbf{k}) = 1 - \Sigma_{1o}^{(h)}(\mathbf{k})$ , then the dressed holon diagonal and off-diagonal Green's functions in Eqs. (29) and (30) can be expressed explicitly as,

$$g(k) = \frac{1}{2} \left( 1 + \frac{\bar{\xi}_{\mathbf{k}}}{E_{\mathbf{k}}} \right) \frac{Z_F(\mathbf{k})}{i\omega_n - E_{\mathbf{k}}} + \frac{1}{2} \left( 1 - \frac{\bar{\xi}_{\mathbf{k}}}{E_{\mathbf{k}}} \right) \frac{Z_F(\mathbf{k})}{i\omega_n + E_{\mathbf{k}}}, \quad (1.31)$$

$$\mathfrak{S}^\dagger(k) = -\frac{Z_F(\mathbf{k})\bar{\Delta}_{hZ}(\mathbf{k})}{2E_{\mathbf{k}}} \left( \frac{1}{i\omega_n - E_{\mathbf{k}}} - \frac{1}{i\omega_n + E_{\mathbf{k}}} \right), \quad (1.32)$$

with  $\bar{\xi}_{\mathbf{k}} = Z_F(\mathbf{k})\xi_{\mathbf{k}}$ ,  $\bar{\Delta}_{hZ}(\mathbf{k}) = Z_F(\mathbf{k})\bar{\Delta}_h(\mathbf{k})$ , and the dressed holon quasiparticle spectrum  $E_{\mathbf{k}} = \sqrt{\bar{\xi}_{\mathbf{k}}^2 + |\bar{\Delta}_{hZ}(\mathbf{k})|^2}$ . Although  $Z_F(\mathbf{k})$  still is a function of  $\mathbf{k}$ , the wave vector dependence is unimportant, since everything happens near the electron Fermi surface. Therefore we need to estimate the special wave vector  $\mathbf{k}_0$  that guarantees  $Z_F = Z_F(\mathbf{k}_0)$  near the electron Fermi surface. In the present charge-spin separation fermion-spin framework [33], the electron diagonal Green's function  $G(i-j, t-t') = \langle\langle C_{i\sigma}(t); C_{j\sigma}^\dagger(t') \rangle\rangle$  is a convolution of the dressed spin Green's function  $D(p)$  and dressed holon

diagonal Green's function  $g(k)$ , and can be evaluated as [33],

$$G(k) = \frac{1}{N} \sum_{\mathbf{p}} \int_{-\infty}^{\infty} \frac{d\omega'}{2\pi} \int_{-\infty}^{\infty} \frac{d\omega''}{2\pi} A_s(\mathbf{p}, \omega') A_h(\mathbf{p} + \mathbf{k}, \omega'') \times \frac{n_F(\omega'') + n_B(\omega')}{i\omega_n + \omega'' - \omega'}, \quad (1.33)$$

where the dressed spin spectral function  $A_s(\mathbf{p}, \omega) = -2\text{Im}D(\mathbf{p}, \omega)$ , the dressed holon spectral function  $A_h(\mathbf{k}, \omega) = -2\text{Im}g(\mathbf{k}, \omega)$ , and  $n_B(\omega)$  and  $n_F(\omega)$  are the boson and fermion distribution functions, respectively. This convolution of the dressed spin Green's function and diagonal dressed holon Green's function reflects the charge-spin recombination [3]. With the help of this electron diagonal Green's function, the electron spectral function  $A(\mathbf{k}, \omega) = -2\text{Im}G(\mathbf{k}, \omega)$  is obtained as,

$$A(\mathbf{k}, \omega) = \frac{1}{N} \sum_{\mathbf{p}} \int_{-\infty}^{\infty} \frac{d\omega'}{2\pi} A_s(\mathbf{p}, \omega') A_h(\mathbf{p} + \mathbf{k}, \omega' + \omega) \times [n_F(\omega' + \omega) + n_B(\omega')]. \quad (1.34)$$

This electron spectral function has been used to extract the electron momentum distribution (then the electron Fermi surface) as [33],

$$n_{\mathbf{k}} = \int_{-\infty}^{\infty} \frac{d\omega}{2\pi} A(\mathbf{k}, \omega) n_F(\omega) = \frac{1}{2} - \frac{1}{N} \sum_{\mathbf{p}} n_s(\mathbf{p}) \int_{-\infty}^{\infty} \frac{d\omega}{2\pi} A_h(\mathbf{p} + \mathbf{k}, \omega) n_F(\omega), \quad (1.35)$$

where

$$n_s(\mathbf{p}) = \int_{-\infty}^{\infty} \frac{d\omega}{2\pi} A_s(\mathbf{p}, \omega) n_B(\omega), \quad (1.36)$$

is the dressed spin momentum distribution. In the present case, this electron momentum distribution can be evaluated explicitly in terms of the mean-field dressed spin Green's function (20) and dressed holon diagonal Green's function (31) as,

$$n_{\mathbf{k}} = \frac{1}{2} - \frac{1}{2N} \sum_{\mathbf{p}} n_s^{(0)}(\mathbf{p}) Z_F(\mathbf{p} - \mathbf{k}) \left( 1 - \frac{\bar{\xi}_{\mathbf{p}-\mathbf{k}}}{E_{\mathbf{p}-\mathbf{k}}} \tanh\left[\frac{1}{2}\beta E_{\mathbf{p}-\mathbf{k}}\right] \right), \quad (1.37)$$

with  $n_s^{(0)}(\mathbf{p}) = B_{\mathbf{p}} \coth(\beta\omega_{\mathbf{p}}/2)/(\omega_{\mathbf{p}})$ . Since the dressed spins center around  $[\pm\pi, \pm\pi]$  in the Brillouin zone in the mean-field level [33], therefore the

above electron momentum distribution can be approximately reduced as  $n_{\mathbf{k}} \approx 1/2 - \rho_s^{(0)} Z_F(\mathbf{k}_{\mathbf{A}} - \mathbf{k}) [1 - \bar{\xi}_{\mathbf{k}_{\mathbf{A}} - \mathbf{k}} \tanh(\beta E_{\mathbf{k}_{\mathbf{A}} - \mathbf{k}}/2) / E_{\mathbf{k}_{\mathbf{A}} - \mathbf{k}}] / 2$ , with  $\mathbf{k}_{\mathbf{A}} = [\pi, \pi]$ , and  $\rho_s^{(0)} = (1/N) \sum_{\mathbf{p}=(\pm\pi, \pm\pi)} n_s^{(0)}(\mathbf{p})$ . It has been shown from the angle resolved photoemission spectroscopy experiments [45] that the electron Fermi surface is small pockets around  $[\pi/2, \pi/2]$  at small doping, and becomes a large electron Fermi surface at large doping. In this case, the Fermi wave vector can be estimated [33] at  $\mathbf{k}_{\mathbf{F}} = [(1-x)\pi/2, (1-x)\pi/2]$ , and its evolution with doping. Now we obtain the wave vector  $\mathbf{k}_0 \approx \mathbf{k}_{\mathbf{A}} - \mathbf{k}_{\mathbf{F}}$  that guarantees  $Z_F(\mathbf{k}_0)$  near the electron Fermi surface, and we only need to calculate  $Z_F = Z_F(\mathbf{k}_0)$  as mentioned above. Since the charge-spin recombination from the convolution of the dressed spin Green's function and dressed holon diagonal Green's function leads to form the electron Fermi surface [3], then the dressed holon single particle coherence  $Z_F$  appearing in the electron momentum distribution also reflects the electron single particle coherence.

Experimentally, some results seem consistent with an s-wave pairing [38], while other measurements gave the evidence in favor of the d-wave pairing [39, 10]. These reflect a fact that the d-wave gap function  $\propto k_x^2 - k_y^2$  belongs to the same representation  $\Gamma_1$  of the orthorhombic crystal group as does s-wave gap function  $\propto k_x^2 + k_y^2$ . For understanding of these experimental results, we consider both s-wave and d-wave cases, i.e.,  $\bar{\Delta}_{hZ}^{(s)}(\mathbf{k}) = \bar{\Delta}_{hZ}^{(s)} \gamma_{\mathbf{k}}^{(s)}$ , with  $\gamma_{\mathbf{k}}^{(s)} = \gamma_{\mathbf{k}} = (\cos k_x + \cos k_y)/2$ , for the s-wave pairing, and  $\bar{\Delta}_{hZ}^{(d)}(\mathbf{k}) = \bar{\Delta}_{hZ}^{(d)} \gamma_{\mathbf{k}}^{(d)}$ , with  $\gamma_{\mathbf{k}}^{(d)} = (\cos k_x - \cos k_y)/2$ , for the d-wave pairing, respectively. In this case, the dressed holon effective gap parameter and single particle coherent weight in Eqs. (27) and (28) satisfy following two equations [20, 21],

$$1 = \frac{1}{N^3} \sum_{\mathbf{k}, \mathbf{q}, \mathbf{p}} (Zt\gamma_{\mathbf{k}+\mathbf{q}} - Zt'\gamma'_{\mathbf{k}+\mathbf{q}})^2 \gamma_{\mathbf{k}-\mathbf{p}+\mathbf{q}}^{(a)} \gamma_{\mathbf{k}}^{(a)} \frac{Z_F^2 B_{\mathbf{q}} B_{\mathbf{p}}}{E_{\mathbf{k}} \omega_{\mathbf{q}} \omega_{\mathbf{p}}} \\ \times \left( \frac{F_1^{(1)}(\mathbf{k}, \mathbf{q}, \mathbf{p})}{(\omega_{\mathbf{p}} - \omega_{\mathbf{q}})^2 - E_{\mathbf{k}}^2} - \frac{F_1^{(2)}(\mathbf{k}, \mathbf{q}, \mathbf{p})}{(\omega_{\mathbf{p}} + \omega_{\mathbf{q}})^2 - E_{\mathbf{k}}^2} \right), \quad (1.38)$$

$$Z_F^{-1} = 1 + \frac{1}{N^2} \sum_{\mathbf{q}, \mathbf{p}} (Zt\gamma_{\mathbf{p}+\mathbf{k}_0} - Zt'\gamma'_{\mathbf{p}+\mathbf{k}_0})^2 Z_F \frac{B_{\mathbf{q}} B_{\mathbf{p}}}{4\omega_{\mathbf{q}} \omega_{\mathbf{p}}} \\ \times \left( \frac{F_2^{(1)}(\mathbf{q}, \mathbf{p})}{(\omega_{\mathbf{p}} - \omega_{\mathbf{q}} - E_{\mathbf{p}-\mathbf{q}+\mathbf{k}_0})^2} + \frac{F_2^{(2)}(\mathbf{q}, \mathbf{p})}{(\omega_{\mathbf{p}} - \omega_{\mathbf{q}} + E_{\mathbf{p}-\mathbf{q}+\mathbf{k}_0})^2} \right. \\ \left. + \frac{F_2^{(3)}(\mathbf{q}, \mathbf{p})}{(\omega_{\mathbf{p}} + \omega_{\mathbf{q}} - E_{\mathbf{p}-\mathbf{q}+\mathbf{k}_0})^2} + \frac{F_2^{(4)}(\mathbf{q}, \mathbf{p})}{(\omega_{\mathbf{p}} + \omega_{\mathbf{q}} + E_{\mathbf{p}-\mathbf{q}+\mathbf{k}_0})^2} \right), \quad (1.39)$$

respectively, where  $a = s, d$ , and

$$F_1^{(1)}(\mathbf{k}, \mathbf{q}, \mathbf{p}) = (\omega_{\mathbf{p}} - \omega_{\mathbf{q}})[n_B(\omega_{\mathbf{q}}) - n_B(\omega_{\mathbf{p}})][1 - 2n_F(E_{\mathbf{k}})] \\ + E_{\mathbf{k}}[n_B(\omega_{\mathbf{p}})n_B(-\omega_{\mathbf{q}}) + n_B(\omega_{\mathbf{q}})n_B(-\omega_{\mathbf{p}})], \quad (1.40)$$

$$F_1^{(2)}(\mathbf{k}, \mathbf{q}, \mathbf{p}) = (\omega_{\mathbf{p}} + \omega_{\mathbf{q}})[n_B(-\omega_{\mathbf{p}}) - n_B(\omega_{\mathbf{q}})][1 - 2n_F(E_{\mathbf{k}})] \\ + E_{\mathbf{k}}[n_B(\omega_{\mathbf{p}})n_B(\omega_{\mathbf{q}}) + n_B(-\omega_{\mathbf{p}})n_B(-\omega_{\mathbf{q}})], \quad (1.41)$$

$$F_2^{(1)}(\mathbf{q}, \mathbf{p}) = n_F(E_{\mathbf{p}-\mathbf{q}+\mathbf{k}_0})[n_B(\omega_{\mathbf{q}}) - n_B(\omega_{\mathbf{p}})] \\ - n_B(\omega_{\mathbf{p}})n_B(-\omega_{\mathbf{q}}), \quad (1.42)$$

$$F_2^{(2)}(\mathbf{q}, \mathbf{p}) = n_F(E_{\mathbf{p}-\mathbf{q}+\mathbf{k}_0})[n_B(\omega_{\mathbf{p}}) - n_B(\omega_{\mathbf{q}})] \\ - n_B(\omega_{\mathbf{q}})n_B(-\omega_{\mathbf{p}}), \quad (1.43)$$

$$F_2^{(3)}(\mathbf{q}, \mathbf{p}) = n_F(E_{\mathbf{p}-\mathbf{q}+\mathbf{k}_0})[n_B(\omega_{\mathbf{q}}) - n_B(-\omega_{\mathbf{p}})] \\ + n_B(\omega_{\mathbf{p}})n_B(\omega_{\mathbf{q}}), \quad (1.44)$$

$$F_2^{(4)}(\mathbf{q}, \mathbf{p}) = n_F(E_{\mathbf{p}-\mathbf{q}+\mathbf{k}_0})[n_B(-\omega_{\mathbf{q}}) - n_B(\omega_{\mathbf{p}})] \\ + n_B(-\omega_{\mathbf{p}})n_B(-\omega_{\mathbf{q}}). \quad (1.45)$$

These two equations (38) and (39) must be solved simultaneously with other self-consistent equations [20],

$$\phi_1 = \frac{1}{2N} \sum_{\mathbf{k}} \gamma_{\mathbf{k}} Z_F \left( 1 - \frac{\bar{\xi}_{\mathbf{k}}}{E_{\mathbf{k}}} \text{th} \left[ \frac{1}{2} \beta E_{\mathbf{k}} \right] \right), \quad (1.46)$$

$$\phi_2 = \frac{1}{2N} \sum_{\mathbf{k}} \gamma'_{\mathbf{k}} Z_F \left( 1 - \frac{\bar{\xi}_{\mathbf{k}}}{E_{\mathbf{k}}} \text{th} \left[ \frac{1}{2} \beta E_{\mathbf{k}} \right] \right), \quad (1.47)$$

$$\delta = \frac{1}{2N} \sum_{\mathbf{k}} Z_F \left( 1 - \frac{\bar{\xi}_{\mathbf{k}}}{E_{\mathbf{k}}} \text{th} \left[ \frac{1}{2} \beta E_{\mathbf{k}} \right] \right), \quad (1.48)$$

$$\chi_1 = \frac{1}{N} \sum_{\mathbf{k}} \gamma_{\mathbf{k}} \frac{B_{\mathbf{k}}}{2\omega_{\mathbf{k}}} \coth \left[ \frac{1}{2} \beta \omega_{\mathbf{k}} \right], \quad (1.49)$$

$$\chi_2 = \frac{1}{N} \sum_{\mathbf{k}} \gamma'_{\mathbf{k}} \frac{B_{\mathbf{k}}}{2\omega_{\mathbf{k}}} \coth \left[ \frac{1}{2} \beta \omega_{\mathbf{k}} \right], \quad (1.50)$$

$$C_1 = \frac{1}{N} \sum_{\mathbf{k}} \gamma_{\mathbf{k}}^2 \frac{B_{\mathbf{k}}}{2\omega_{\mathbf{k}}} \coth \left[ \frac{1}{2} \beta \omega_{\mathbf{k}} \right], \quad (1.51)$$

$$C_2 = \frac{1}{N} \sum_{\mathbf{k}} \gamma_{\mathbf{k}}'^2 \frac{B_{\mathbf{k}}}{2\omega_{\mathbf{k}}} \coth \left[ \frac{1}{2} \beta \omega_{\mathbf{k}} \right], \quad (1.52)$$

$$C_3 = \frac{1}{N} \sum_{\mathbf{k}} \gamma_{\mathbf{k}} \gamma'_{\mathbf{k}} \frac{B_{\mathbf{k}}}{2\omega_{\mathbf{k}}} \coth \left[ \frac{1}{2} \beta \omega_{\mathbf{k}} \right], \quad (1.53)$$

$$\frac{1}{2} = \frac{1}{N} \sum_{\mathbf{k}} \frac{B_{\mathbf{k}}}{2\omega_{\mathbf{k}}} \coth\left[\frac{1}{2}\beta\omega_{\mathbf{k}}\right], \quad (1.54)$$

$$\chi_1^z = \frac{1}{N} \sum_{\mathbf{k}} \gamma_{\mathbf{k}} \frac{B_z(\mathbf{k})}{2\omega_z(\mathbf{k})} \coth\left[\frac{1}{2}\beta\omega_z(\mathbf{k})\right], \quad (1.55)$$

$$\chi_2^z = \frac{1}{N} \sum_{\mathbf{k}} \gamma'_{\mathbf{k}} \frac{B_z(\mathbf{k})}{2\omega_z(\mathbf{k})} \coth\left[\frac{1}{2}\beta\omega_z(\mathbf{k})\right], \quad (1.56)$$

$$C_1^z = \frac{1}{N} \sum_{\mathbf{k}} \gamma_{\mathbf{k}}^2 \frac{B_z(\mathbf{k})}{2\omega_z(\mathbf{k})} \coth\left[\frac{1}{2}\beta\omega_z(\mathbf{k})\right], \quad (1.57)$$

$$C_3^z = \frac{1}{N} \sum_{\mathbf{k}} \gamma_{\mathbf{k}} \gamma'_{\mathbf{k}} \frac{B_z(\mathbf{k})}{2\omega_z(\mathbf{k})} \coth\left[\frac{1}{2}\beta\omega_z(\mathbf{k})\right], \quad (1.58)$$

then all the order parameters, decoupling parameter  $\alpha$ , and chemical potential  $\mu$  are determined by the self-consistent calculation [20]. With above discussions, we now can obtain the dressed holon pair gap function in terms of the off-diagonal Green's function (32) as,

$$\Delta_h^{(a)}(\mathbf{k}) = -\frac{1}{\beta} \sum_{i\omega_n} \mathfrak{S}^\dagger(\mathbf{k}, i\omega_n) = \frac{1}{2} Z_F \frac{\bar{\Delta}_{hZ}^{(a)}(\mathbf{k})}{E_{\mathbf{k}}} \tanh\left[\frac{1}{2}\beta E_{\mathbf{k}}\right], \quad (1.59)$$

then the dressed holon pair order parameter in Eq. (9) can be evaluated explicitly from this dressed holon pair gap function (59) as,

$$\Delta_h^{(a)} = \frac{2}{N} \sum_{\mathbf{k}} [\gamma_{\mathbf{k}}^{(a)}]^2 \frac{Z_F \bar{\Delta}_{hZ}^{(a)}}{E_{\mathbf{k}}} \tanh\left[\frac{1}{2}\beta E_{\mathbf{k}}\right]. \quad (1.60)$$

In the charge-spin separation fermion-spin theory, we [20] have shown that the dressed holon pairing state originating from the kinetic energy terms by exchanging dressed spin excitations also leads to form the electron Cooper pairing state, and the superconducting gap function is obtained from the electron off-diagonal Green's function  $\Gamma^\dagger(i-j, t-t') = \langle\langle C_{i\uparrow}^\dagger(t); C_{j\downarrow}^\dagger(t') \rangle\rangle$ , which is a convolution of the dressed spin Green's function and dressed holon off-diagonal Green's function and reflects the charge-spin recombination [3]. In the present case, it can be evaluated in terms of the mean-field dressed spin Green's function (20) and dressed holon off-diagonal Green's function (32) as,

$$\begin{aligned} \Gamma^\dagger(k) &= \frac{1}{N} \sum_{\mathbf{p}} \frac{Z_F \bar{\Delta}_{hZ}^{(a)}(\mathbf{p}-\mathbf{k})}{E_{\mathbf{p}-\mathbf{k}}} \frac{B_{\mathbf{p}}}{2\omega_{\mathbf{p}}} \left( \frac{(\omega_{\mathbf{p}} + E_{\mathbf{p}-\mathbf{k}})[n_B(\omega_{\mathbf{p}}) + n_F(-E_{\mathbf{p}-\mathbf{k}})]}{(i\omega_n)^2 - (\omega_{\mathbf{p}} + E_{\mathbf{p}-\mathbf{k}})^2} \right. \\ &\quad \left. - \frac{(\omega_{\mathbf{p}} - E_{\mathbf{p}-\mathbf{k}})[n_B(\omega_{\mathbf{p}}) + n_F(E_{\mathbf{p}-\mathbf{k}})]}{(i\omega_n)^2 - (\omega_{\mathbf{p}} - E_{\mathbf{p}-\mathbf{k}})^2} \right). \end{aligned} \quad (1.61)$$

then the superconducting gap function is obtained from this electron off-diagonal Green's function as,

$$\Delta^{(a)}(\mathbf{k}) = -\frac{1}{N} \sum_{\mathbf{p}} \frac{Z_F \bar{\Delta}_h^{(a)}(\mathbf{p} - \mathbf{k})}{2E_{\mathbf{p}-\mathbf{k}}} \tanh\left[\frac{1}{2}\beta E_{\mathbf{p}-\mathbf{k}}\right] \frac{B_{\mathbf{p}}}{2\omega_{\mathbf{p}}} \coth\left[\frac{1}{2}\beta\omega_{\mathbf{p}}\right], \quad (1.62)$$

which shows that the symmetry of the electron Cooper pair is essentially determined by the symmetry of the dressed holon pair. From this superconducting gap function (62), the superconducting gap parameter in Eq. (8) is obtained in terms of Eqs. (60) and (49) as  $\Delta^{(a)} = -\chi_1 \Delta_h^{(a)}$ . However, in contrast with the conventional superconductors, the dressed holon (then electron) pairing interaction in cuprate superconductors is also doping dependent, therefore the experimental observed superconducting gap parameter in cuprate superconductors should be the effective superconducting gap parameter  $\bar{\Delta}^{(a)} \sim -\chi_1 \bar{\Delta}_h^{(a)}$ , which measures the strength of the binding of electrons into electron Cooper pairs. In Fig. 1, we plot the effective dressed holon pairing (a) and effective superconducting (b) gap parameters in the s-wave symmetry (solid line) and d-wave symmetry (dashed line) as a function of the hole doping concentration  $x$  at  $T = 0.002J$  for  $t/J = 2.5$  and  $t'/J = 0.3$ . For comparison, the experimental result [40] of the upper critical field as a function of the hole doping concentration is also shown in Fig. 1(b). In a given doping concentration, the upper critical field is defined as the critical field that destroys the superconducting-state at the zero temperature, therefore the upper critical field also measures the strength of the binding of electrons into Cooper pairs like the effective superconducting gap parameter [40]. In other words, both effective superconducting gap parameter and upper critical field have a similar doping dependence [40]. In this sense, our result is in good agreement with the experimental data [40]. In particular, the value of  $\bar{\Delta}^{(d)}$  increases with increasing doping in the underdoped regime, and reaches a maximum in the optimal doping  $x_{\text{opt}} \approx 0.15$ , then decreases in the overdoped regime. Since the effective dressed holon pairing gap parameter measures the strength of the binding of dressed holons into dressed holon pairs, then our results also show that although the superconductivity is driven by the kinetic energy by exchanging dressed spin excitations, the strength of the binding of electrons into electron Cooper pairs is still suppressed by the short-range antiferromagnetic fluctuation.

Now we turn to discuss the superconducting transition temperature. The present result in Eq. (62) also shows that the superconducting transition temperature  $T_c^{(a)}$  occurring in the case of the superconducting gap parameter  $\Delta^{(a)} = 0$  is identical to the dressed holon pair transition temperature



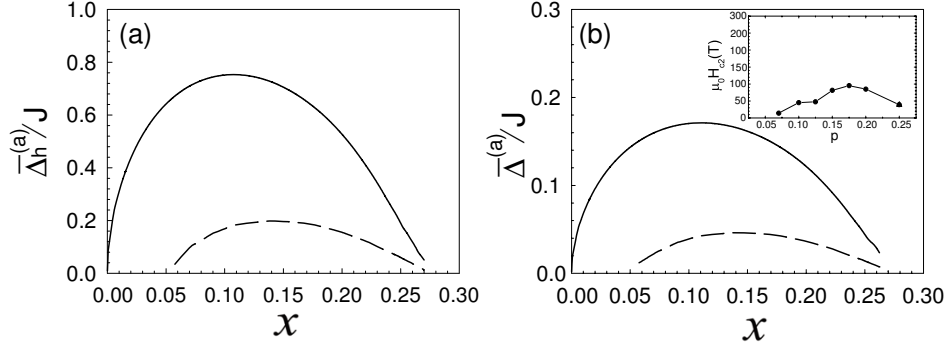


Figure 1.1: The effective dressed holon pairing (a) and effective superconducting (b) gap parameters in the s-wave symmetry (solid line) and d-wave symmetry (dashed line) as a function of the hole doping concentration in  $T = 0.002J$  for  $t/J = 2.5$  and  $t'/t = 0.3$ . Inset: the experimental result of the upper critical field as a function of the hole doping concentration taken from Ref. [40].

occurring in the case of the effective holon pairing gap parameter  $\bar{\Delta}_{hZ}^{(a)} = 0$ . In this case, we have performed a calculation for the doping dependence of the superconducting transition temperature, and the result of the superconducting transition temperature  $T_c^{(a)}$  as a function of the hole doping concentration  $x$  in the s-wave symmetry (solid line) and d-wave symmetry (dashed line) for  $t/J = 2.5$  and  $t'/J = 0.3$  is plotted in Fig. 2 in comparison with the experimental result [7] (inset). Our result shows that for the s-wave symmetry, the maximal superconducting transition temperature  $T_c^{(s)}$  occurs around a particular doping concentration  $x \approx 0.10$ , and then decreases in both lower doped and higher doped regimes. However, for the d-wave symmetry, the maximal superconducting transition temperature  $T_c^{(d)}$  occurs around the optimal doping concentration  $x_{\text{opt}} \approx 0.15$ , and then decreases in both underdoped and overdoped regimes. Although the superconducting pairing symmetry is doping dependent, the superconducting state has the d-wave symmetry in a wide range of doping, in good agreement with the experiments [11, 41, 42]. Furthermore,  $T_c^{(d)}$  in the underdoped regime ( $T_c^{(s)}$  in the lower doped regime) is proportional to the hole doping concentration  $x$ , and therefore  $T_c^{(d)}$  in the underdoped regime ( $T_c^{(s)}$  in the lower doped regime) is set by the hole doping concentration [43]. This reflects that the density of the dressed holons directly determines the superfluid density

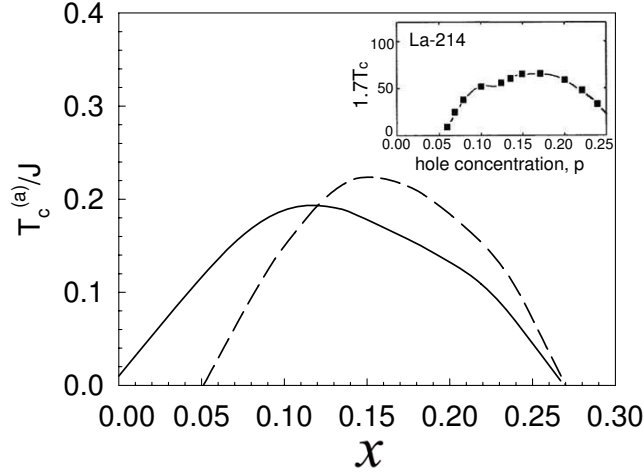


Figure 1.2: The superconducting transition temperature as a function of the hole doping concentration in the s-wave symmetry (solid line) and d-wave symmetry (dashed line) for  $t/J = 2.5$  and  $t'/t = 0.3$ . Inset: the experimental result taken from Ref. [7].

in the underdoped regime for the d-wave case (the lower doped regime for the s-wave case). Using an reasonable estimative value of  $J \sim 800\text{K}$  to  $1200\text{K}$  in doped cuprates [44], the superconducting transition temperature in the optimal doping is  $T_c^{(d)} \approx 0.22J \approx 176\text{K} \sim 264\text{K}$ , in semiquantitative agreement with the experimental data [7, 42, 43]. In comparison with the previous result based on the  $t$ - $J$  model [21], our present result of the  $t$ - $t'$ - $J$  model also shows that the effect of the additional second neighbor hopping  $t'$  is to enhance the d-wave superconducting pairing correlation, and suppress the s-wave superconducting pairing correlation.

Since cuprates superconductors are highly anisotropic materials, therefore the electron spectral function  $A(\mathbf{k}, \omega)$  is dependent on the in-plane momentum [45]. Although the electron spectral function in doped cuprates obtained from the angle resolved photoemission spectroscopy is very broad in the normal-state, indicating that there are no quasiparticles. However, in the superconducting-state, the full energy dispersion of quasiparticles has been observed [46]. According to a comparison of the density of states as measured by scanning tunnelling microscopy [47] and angle resolved photoemission spectroscopy spectral function [6, 45] at  $[\pi, 0]$  point on identical samples, it has been shown that the most contributions of the angle-integrated

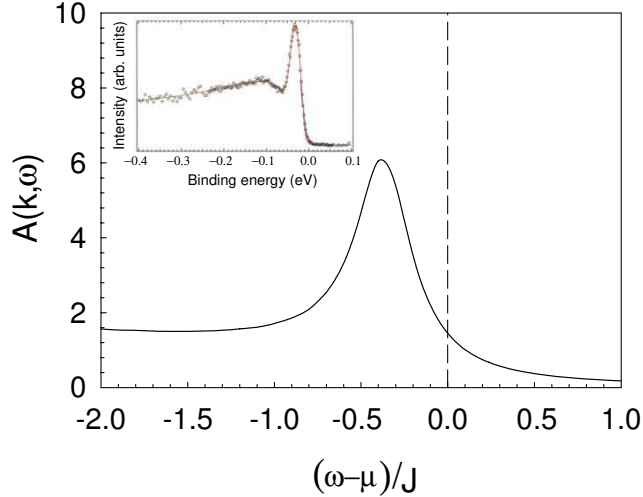


Figure 1.3: The electron spectral function with the d-wave symmetry at  $[\pi, 0]$  point in  $x_{\text{opt}} = 0.15$  and  $T = 0.002J$  for  $t/J = 2.5$  and  $t'/J = 0.3$ . Inset: the experimental result taken from Ref. [6].

spectral function come from  $[\pi, 0]$  point. In addition, the d-wave gap, and therefore the electron pairing energy scale, is maximized at  $[\pi, 0]$  point. Although the sharp superconducting quasiparticle peak at  $[\pi, 0]$  point in cuprate superconductors has been widely studied, the origin and its implications are still under debate [46]. Within the present theoretical framework of superconductivity, we have discussed this issue, and the result of the electron spectral function (34) with the d-wave symmetry at  $[\pi, 0]$  point in the optimal doping  $x_{\text{opt}} = 0.15$  and temperature  $T = 0.002J$  for  $t/J = 2.5$  and  $t'/J = 0.3$  is plotted in Fig. 3 in comparison with the experimental result [6] (inset). Our result shows that the position of the peak of the electron spectral function in  $[\pi, 0]$  point is located at  $\omega_{\text{peak}} \approx 0.4J \approx 0.028\text{eV} \sim 0.04\text{eV}$ , which is quantitatively consistent with the  $\omega_{\text{peak}} \approx 0.03\text{eV}$  observed [6] in the cuprate superconductor  $\text{Bi}_2\text{Sr}_2\text{CaCu}_2\text{O}_{8+x}$ . Furthermore, we have discussed the temperature dependence of the electron spectral function and overall quasiparticle dispersion, and these and related theoretical results will be presented elsewhere.

The essential physics of superconductivity in the present  $t$ - $t'$ - $J$  model is the same as that in the  $t$ - $J$  model [20, 21]. The antisymmetric part of the self-energy function  $\Sigma_{1o}^{(h)}(\mathbf{k})$  (then  $Z_F$ ) describes the single particle (quasiparticle) coherence, and therefore  $Z_F$  is closely related to the quasiparticle

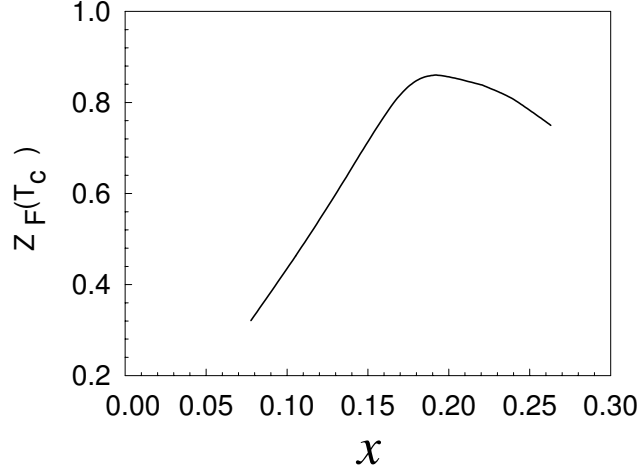


Figure 1.4: The single particle coherent weight  $Z_F(T_c)$  as a function of the hole doping concentration for  $t/J = 2.5$  and  $t'/t = 0.3$ .

density, while the self-energy function  $\Sigma_2^{(h)}(\mathbf{k})$  describes the effective dressed holon pairing gap function. In particular, both  $Z_F$  and  $\Sigma_2^{(h)}(\mathbf{k})$  are doping and temperature dependent. Since the superconducting-order is established through an emerging quasiparticle [6], therefore the superconducting-order is controlled by both gap function and quasiparticle coherence, and is reflected explicitly in the self-consistent equations (38) and (39). To show this point clearly, we plot the single particle (quasiparticle) coherent weight  $Z_F(T_c)$  as a function of the hole doping concentration  $x$  for  $t/J = 2.5$  and  $t'/t = 0.3$  in Fig. 4. As seen from Fig. 4, the doping dependent behavior of the single particle coherent weight resembles that of the superfluid density in cuprate superconductors, i.e.,  $Z_F(T_c)$  grows linearly with the hole doping concentration in the underdoped and optimally doped regimes, and then decreases with increasing doping in the overdoped regime, which leads to that the superconducting transition temperature reaches a maximum in the optimal doping, and then decreases in both underdoped and overdoped regimes. Since the effective superconducting gap function  $\bar{\Delta}^{(s)}(\mathbf{k}) = \bar{\Delta}^{(s)}(\cos k_x + \cos k_y)/2$  for the s-wave symmetry or  $\bar{\Delta}^{(d)}(\mathbf{k}) = \bar{\Delta}^{(d)}(\cos k_x - \cos k_y)/2$  for the d-wave case is dependent on the momentum and the most contributions of the electronic states come from  $[\pi, 0]$  point [6], therefore although the value of the effective superconducting gap parameter  $\bar{\Delta}^{(s)}$  (then the ratio  $\bar{\Delta}^{(s)}/T_c^{(s)}$ ) for the s-wave symmetry is larger than these  $\bar{\Delta}^{(d)}$  (then the ratio  $\bar{\Delta}^{(d)}/T_c^{(d)}$ )

in the d-wave case, the system has the superconducting transition temperature  $T_c^{(d)}$  with the d-wave symmetry in a wide range of doping. Although the superconducting state is characterized by the charge-spin recombination, the superconducting transition temperature is determined by the dressed holon pairing transition temperature. This is why the superfluid density in the underdoped regime vanishes more or less linearly with the hole doping concentration [43], and the cuprate superconductors are the gossamer superconductors. Moreover, the dressed holon pairs condense with the d-wave symmetry in a wide range of doping in the present framework of superconductivity, then the electron Cooper pairs originating from the dressed holon pairing state are due to the charge-spin recombination, and their condensation automatically gives the electron quasiparticle character. Our results also show that the superconducting-state of cuprate superconductors is the conventional Bardeen-Cooper-Schrieffer like, so that some of the basic Bardeen-Cooper-Schrieffer formalism [8] is still valid in discussions of the doping dependence of the effective superconducting gap parameter and superconducting transition temperature, and electron spectral function [46], although the pairing mechanism is driven by the kinetic energy by exchanging dressed spin excitations, and other exotic properties, such as the incommensurate magnetic scattering and commensurate  $[\pi, \pi]$  resonance in the superconducting-state discussed in the following section, are beyond Bardeen-Cooper-Schrieffer theory.

### 1.3 Doping and energy dependent incommensurate magnetic scattering and commensurate resonance

Experimentally, by virtue of systematic studies using the nuclear magnetic resonance, and muon spin rotation techniques, particularly the inelastic neutron scattering, the doping and energy dependent magnetic excitation spectrum in doped cuprates in the superconducting-state have been well established: (a) at low energy, the incommensurate magnetic scattering peaks are shifted from the antiferromagnetic wave vector  $[\pi, \pi]$  to four points  $[(1 \pm \delta)\pi, \pi]$  and  $[\pi, (1 \pm \delta)\pi]$  with  $\delta$  as the incommensurability parameter [12, 13, 14]; (b) then with increasing energy these incommensurate magnetic scattering peaks are converged on the commensurate  $[\pi, \pi]$  resonance peak at intermediate energy [13, 26, 27, 24]; and (c) well above this resonance energy, the continuum of magnetic excitations peaked at the incommensurate

positions  $[(1 \pm \delta)\pi, (1 \pm \delta)\pi]$  in the diagonal direction are observed [15, 25]. It has been emphasized that the geometry of these incommensurate magnetic excitations is two-dimensional [48, 15]. Although some of these magnetic properties have been observed in the normal-state, these incommensurate magnetic scattering and commensurate  $[\pi, \pi]$  resonance are the main new feature that appears into the superconducting-state.

In the charge-spin separation fermion-spin theory, the magnetic fluctuation is dominated by the scattering of the dressed spins [19, 49]. Since in the normal-state the dressed spins move in the dressed holon background, therefore the dressed spin self-energy (then full dressed spin Green's function) in the normal-state has been obtained in terms of the collective mode in the dressed holon particle-hole channel [19, 49]. With the help of this full dressed spin Green's function in the normal-state, the incommensurate magnetic scattering and integrated spin response of doped cuprates in the normal-state have been discussed [19, 49], and the results of the doping dependence of the incommensurability and integrated dynamical spin susceptibility are consistent with the experimental results in the normal-state [5, 12, 13]. However, in the present superconducting-state discussed in section 2, the antiferromagnetic fluctuation has been incorporated into the electron off-diagonal Green's function (61) (hence the electron Cooper pair) in terms of the dressed spin Green's function, therefore there is a coexistence of the electron Cooper pair and antiferromagnetic short-range correlation, and then antiferromagnetic short-range correlation can persist into superconductivity [20]. Moreover, in the superconducting-state, the dressed spins move in the dressed holon pair background. In this case, we calculate the dressed spin self-energy (then the full dressed spin Green's function) in the superconducting-state in terms of the collective mode in the dressed holon particle-particle channel, and then give a quantitative explanation of the incommensurate magnetic scattering peaks at both low and high energies [13, 12, 15, 25] and commensurate  $[\pi, \pi]$  resonance peak at intermediate energy [26, 27, 24] in the superconducting-state.

Following our previous discussions for the normal-state case [19, 49], the full dressed spin Green's function in the present superconducting-state is obtained as,

$$D(\mathbf{k}, \omega) = \frac{1}{D^{(0)-1}(\mathbf{k}, \omega) - \Sigma^{(s)}(\mathbf{k}, \omega)}, \quad (1.63)$$

with the second order dressed spin self-energy  $\Sigma^{(s)}(\mathbf{k}, \omega)$ . Within the framework of the equation of motion method [19, 49], this dressed spin self-energy in the superconducting-state with the d-wave symmetry can be obtained

from the dressed holon bubble in the dressed holon particle-particle channel as,

$$\Sigma_s(k) = \frac{1}{N^2} \sum_{\mathbf{p}, \mathbf{q}} \Lambda(\mathbf{q}, \mathbf{p}, \mathbf{k}) \frac{1}{\beta} \sum_{iq_m} D^{(0)}(q+k) \frac{1}{\beta} \sum_{ip_m} \mathfrak{S}^\dagger(p) \mathfrak{S}(p+q), \quad (1.64)$$

where  $\Lambda(\mathbf{q}, \mathbf{p}, \mathbf{k}) = [(Zt\gamma_{\mathbf{k}-\mathbf{p}} - Zt'\gamma'_{\mathbf{k}-\mathbf{p}})^2 + (Zt\gamma_{\mathbf{q}+\mathbf{p}+\mathbf{k}} - Zt'\gamma'_{\mathbf{q}+\mathbf{p}+\mathbf{k}})^2]$ . This dressed spin self-energy (64) can be evaluated explicitly in terms of the dressed holon off-diagonal Green's function (32) and dressed spin mean-field Green's function (20) as,

$$\begin{aligned} \Sigma_s(\mathbf{k}, \omega) &= \frac{1}{N^2} \sum_{\mathbf{p}, \mathbf{q}} \Lambda(\mathbf{q}, \mathbf{p}, \mathbf{k}) \frac{B_{\mathbf{q}+\mathbf{k}} Z_F^2 \bar{\Delta}_{hZ}^{(a)}(\mathbf{p}) \bar{\Delta}_{hZ}^{(a)}(\mathbf{p}+\mathbf{q})}{\omega_{\mathbf{q}+\mathbf{k}} 4 E_{\mathbf{p}} E_{\mathbf{p}+\mathbf{q}}} \\ &\times \left( \frac{F_s^{(1)}(\mathbf{k}, \mathbf{p}, \mathbf{q})}{\omega^2 - (E_{\mathbf{p}} - E_{\mathbf{p}+\mathbf{q}} + \omega_{\mathbf{q}+\mathbf{k}})^2} + \frac{F_s^{(2)}(\mathbf{k}, \mathbf{p}, \mathbf{q})}{\omega^2 - (E_{\mathbf{p}+\mathbf{q}} - E_{\mathbf{p}} + \omega_{\mathbf{q}+\mathbf{k}})^2} \right. \\ &+ \frac{F_s^{(3)}(\mathbf{k}, \mathbf{p}, \mathbf{q})}{\omega^2 - (E_{\mathbf{p}} + E_{\mathbf{p}+\mathbf{q}} + \omega_{\mathbf{q}+\mathbf{k}})^2} \\ &\left. + \frac{F_s^{(4)}(\mathbf{k}, \mathbf{p}, \mathbf{q})}{\omega^2 - (E_{\mathbf{p}+\mathbf{q}} + E_{\mathbf{p}} - \omega_{\mathbf{q}+\mathbf{k}})^2} \right), \quad (1.65) \end{aligned}$$

where

$$\begin{aligned} F_s^{(1)}(\mathbf{k}, \mathbf{p}, \mathbf{q}) &= (E_{\mathbf{p}} - E_{\mathbf{p}+\mathbf{q}} + \omega_{\mathbf{q}+\mathbf{k}}) \{n_B(\omega_{\mathbf{q}+\mathbf{k}}) [n_F(E_{\mathbf{p}}) - n_F(E_{\mathbf{p}+\mathbf{q}})] \\ &- n_F(E_{\mathbf{p}+\mathbf{q}}) n_F(-E_{\mathbf{p}})\}, \quad (1.66) \end{aligned}$$

$$\begin{aligned} F_s^{(2)}(\mathbf{k}, \mathbf{p}, \mathbf{q}) &= (E_{\mathbf{p}+\mathbf{q}} - E_{\mathbf{p}} + \omega_{\mathbf{q}+\mathbf{k}}) \{n_B(\omega_{\mathbf{q}+\mathbf{k}}) [n_F(E_{\mathbf{p}+\mathbf{q}}) - n_F(E_{\mathbf{p}})] \\ &- n_F(E_{\mathbf{p}}) n_F(-E_{\mathbf{p}+\mathbf{q}})\}, \quad (1.67) \end{aligned}$$

$$\begin{aligned} F_s^{(3)}(\mathbf{k}, \mathbf{p}, \mathbf{q}) &= (E_{\mathbf{p}} + E_{\mathbf{p}+\mathbf{q}} + \omega_{\mathbf{q}+\mathbf{k}}) \{n_B(\omega_{\mathbf{q}+\mathbf{k}}) [n_F(-E_{\mathbf{p}}) - n_F(E_{\mathbf{p}+\mathbf{q}})] \\ &+ n_F(-E_{\mathbf{p}+\mathbf{q}}) n_F(-E_{\mathbf{p}})\}, \quad (1.68) \end{aligned}$$

$$\begin{aligned} F_s^{(4)}(\mathbf{k}, \mathbf{p}, \mathbf{q}) &= (E_{\mathbf{p}} + E_{\mathbf{p}+\mathbf{q}} - \omega_{\mathbf{q}+\mathbf{k}}) \{n_B(\omega_{\mathbf{q}+\mathbf{k}}) [n_F(-E_{\mathbf{p}}) - n_F(E_{\mathbf{p}+\mathbf{q}})] \\ &- n_F(E_{\mathbf{p}+\mathbf{q}}) n_F(E_{\mathbf{p}})\}. \quad (1.69) \end{aligned}$$

With the help of this full dressed spin Green's function (63), we can obtain the dynamical spin structure factor in the superconducting-state with the d-wave symmetry as,

$$\begin{aligned} S(\mathbf{k}, \omega) &= -2[1 + n_B(\omega)] \text{Im}D(\mathbf{k}, \omega) \\ &= -\frac{2[1 + n_B(\omega)] B_{\mathbf{k}}^2 \text{Im}\Sigma_s(\mathbf{k}, \omega)}{[\omega^2 - \omega_{\mathbf{k}}^2 - B_{\mathbf{k}} \text{Re}\Sigma_s(\mathbf{k}, \omega)]^2 + [B_{\mathbf{k}} \text{Im}\Sigma_s(\mathbf{k}, \omega)]^2}, \quad (1.70) \end{aligned}$$

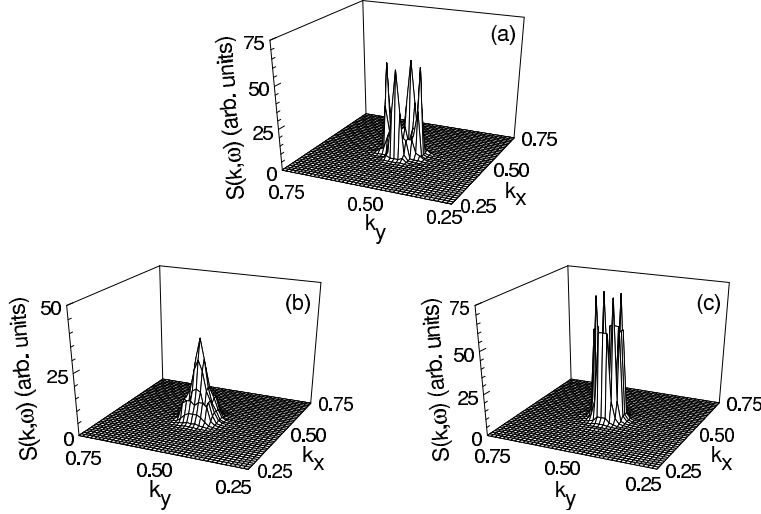


Figure 1.5: The dynamical spin structure factor  $S(\mathbf{k}, \omega)$  in the  $(k_x, k_y)$  plane at  $x_{\text{opt}} = 0.15$  with  $T = 0.002J$  for  $t/J = 2.5$  and  $t'/t = 0.3$  at (a)  $\omega = 0.12J$ , (b)  $\omega = 0.4J$ , and (c)  $\omega = 0.82J$ .

where  $\text{Im}\Sigma_s(\mathbf{k}, \omega)$  and  $\text{Re}\Sigma_s(\mathbf{k}, \omega)$  are the imaginary and real parts of the second order spin self-energy (65), respectively.

We are now ready to discuss the doping and energy dependent magnetic excitation spectrum of doped cuprates in the superconducting-state. In Fig. 5, we plot the dynamical spin structure factor  $S(\mathbf{k}, \omega)$  in the  $(k_x, k_y)$  plane at the optimal doping  $x_{\text{opt}} = 0.15$  with temperature  $T = 0.002J$  for parameters  $t/J = 2.5$  and  $t'/t = 0.3$  at energy (a)  $\omega = 0.12J$ , (b)  $\omega = 0.4J$ , and (c)  $\omega = 0.82J$ . Our result shows that the distinct feature is the presence of the incommensurate-commensurate-incommensurate transition in the spin fluctuation geometry. At low energy, the incommensurate magnetic scattering peaks are located at  $[(1 \pm \delta)/2, 1/2]$  and  $[1/2, (1 \pm \delta)/2]$  (hereafter we use the units of  $[2\pi, 2\pi]$ ). However, these incommensurate magnetic scattering peaks are energy dependent, i.e., although these magnetic scattering peaks retain the incommensurate pattern at  $[(1 \pm \delta)/2, 1/2]$  and  $[1/2, (1 \pm \delta)/2]$  at low energy, the positions of these incommensurate magnetic scattering peaks move towards  $[1/2, 1/2]$  with increasing energy, and then the commensurate  $[1/2, 1/2]$  resonance peak appears at intermediate energy  $\omega_r = 0.4J$ . This anticipated resonance energy  $\omega_r = 0.4J \approx 40$  meV [44] is in quantitative agreement with the resonance energy  $\approx 41$  meV observed in the optimally



doped  $\text{YBa}_2\text{Cu}_3\text{O}_{6+y}$  [13, 26, 27, 24]. Furthermore, the incommensurate magnetic scattering peaks are separated again above the commensurate resonance energy, and all incommensurate magnetic scattering peaks lie on a circle of radius of  $\delta'$  at high energy. In particular, the values of  $\delta'$  at high energy are different from the corresponding values of  $\delta$  at low energy. Although some incommensurate satellite parallel peaks appear, the main weight of the incommensurate magnetic scattering peaks is in the diagonal direction. Moreover, the separation at high energy gradually increases with increasing energy although the peaks have a weaker intensity than those below the commensurate resonance energy. To show this point clearly, we plot the evolution of the magnetic scattering peaks with energy at  $x_{\text{opt}} = 0.15$  in Fig. 6. For comparison, the experimental result [24] of  $\text{YBa}_2\text{Cu}_3\text{O}_{6+y}$  with  $y = 0.7$  ( $x \approx 0.12$ ) in the superconducting-state is also shown in the same figure. The similar experimental results [27, 15] have also been obtained for  $\text{YBa}_2\text{Cu}_3\text{O}_{6+y}$  with different doping concentrations. Our theoretical results show that there is a narrow energy range for the commensurate resonance peak. The similar narrow energy range for the commensurate resonance peak has been observed from experiments [27]. Our results also show that in contrast to the case at low energy, the magnetic excitations at high energy disperse almost linearly with energy [24, 15, 25]. For a better understanding of the commensurate resonance, we have discussed the doping dependence of the commensurate resonance, and the result of the resonance energy  $\omega_r$  as a function of doping  $x - x_{\text{opt}}$  in  $T = 0.002J$  for  $t/J = 2.5$  and  $t'/t = 0.3$  is plotted in Fig. 7 in comparison with the experimental result [26] (inset). It is shown that in analogy to the doping dependence of the superconducting transition temperature, the magnetic resonance energy  $\omega_r$  increases with increasing doping in the underdoped regime, and reaches a maximum in the optimal doping, then decreases in the overdoped regime. These mediating dressed spin excitations in the superconducting-state are coupled to the conducting dressed holons (then electrons) under the kinetic energy driven superconducting mechanism [20], and have energy greater than the dressed holon pairing energy (then Cooper pairing energy). Furthermore, we have also made a series of scans for  $S(\mathbf{k}, \omega)$  at different temperatures, and found that those unusual magnetic excitations are present near the superconducting transition temperature. These results are quantitatively consistent with the major experimental observations of doped cuprates in the superconducting-state [13, 26, 27, 24, 15, 25].

The physical interpretation to the above obtained results can be found from the property of the renormalized dressed spin excitation spectrum  $\Omega_{\mathbf{k}}^2 = \omega_{\mathbf{k}}^2 + \text{Re}\Sigma^{(s)}(\mathbf{k}, \Omega_{\mathbf{k}})$  in Eq. (70). Since both mean-field dressed spin excitation

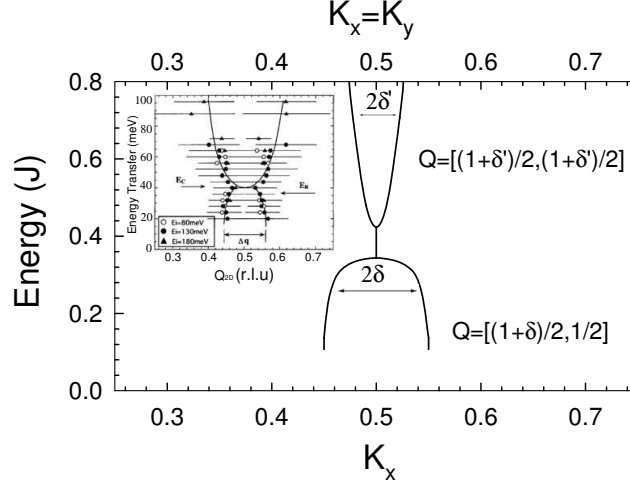


Figure 1.6: The energy dependence of the position of the magnetic scattering peaks at  $x_{\text{opt}} = 0.15$  and  $T = 0.002J$  for  $t/J = 2.5$  and  $t'/t = 0.3$ . Inset: the experimental result on  $\text{YBa}_2\text{Cu}_3\text{O}_{6.85}$  in the superconducting-state taken from Ref. [24].

spectrum  $\omega_{\mathbf{k}}$  and dressed spin self-energy function  $\Sigma^{(s)}(\mathbf{k}, \omega)$  in Eq. (65) are strong doping and energy dependent, this leads to that the renormalized dressed spin excitation spectrum also is strong doping and energy dependent. The dynamical spin structure factor in Eq. (70) has a well-defined resonance character, where  $S(\mathbf{k}, \omega)$  exhibits peaks when the incoming neutron energy  $\omega$  is equal to the renormalized spin excitation, i.e.,

$$W(\mathbf{k}_c, \omega) \equiv [\omega^2 - \omega_{\mathbf{k}_c}^2 - B_{\mathbf{k}_c} \text{Re}\Sigma^{(s)}(\mathbf{k}_c, \omega)]^2 = [\omega^2 - \Omega_{\mathbf{k}_c}^2]^2 \sim 0, \quad (1.71)$$

for certain critical wave vectors  $\mathbf{k}_c = \mathbf{k}_c^{(L)}$  at low energy,  $\mathbf{k}_c = \mathbf{k}_c^{(I)}$  at intermediate energy, and  $\mathbf{k}_c = \mathbf{k}_c^{(H)}$  at high energy, then the weight of these peaks is dominated by the inverse of the imaginary part of the dressed spin self-energy  $1/\text{Im}\Sigma^{(s)}(\mathbf{k}_c^{(L)}, \omega)$  at low energy,  $1/\text{Im}\Sigma^{(s)}(\mathbf{k}_c^{(I)}, \omega)$  at intermediate energy, and  $1/\text{Im}\Sigma^{(s)}(\mathbf{k}_c^{(H)}, \omega)$  at high energy, respectively. In the normal-state [19, 49], the dressed holon energy spectrum has one branch  $\xi_{\mathbf{k}}$ , while in the present superconducting-state, the dressed holon quasiparticle spectrum has two branches  $\pm E_{\mathbf{k}}$ , this leads to that the dressed spin self-energy function  $\Sigma^{(s)}(\mathbf{k}, \omega)$  in Eq. (65) is rather complicated, where there are four terms in the right side of Eq. (65). In comparison with the normal-state case [19, 49], the contribution for the first and second terms in the right side of the dressed

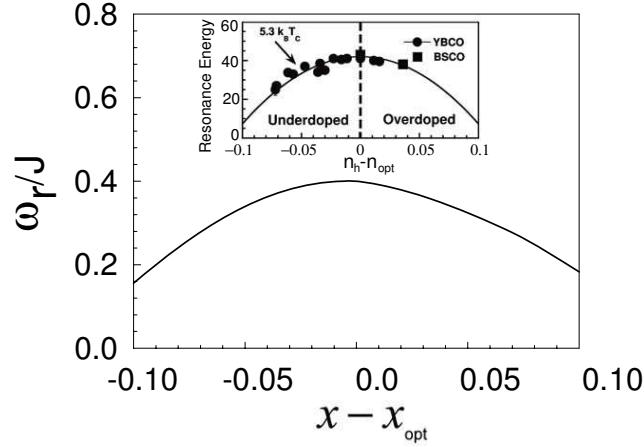


Figure 1.7: The resonance energy  $\omega_r$  as a function of  $x - x_{\text{opt}}$  with  $T = 0.002J$  for  $t/J = 2.5$  and  $t'/t = 0.3$ . Inset: the experimental result taken from Ref. [26].

spin self-energy (65) comes from the lower band  $-E_{\mathbf{k}}$  of the dressed holon quasiparticle spectrum like the normal-state case, while the contribution for the third and fourth terms in the right side of the dressed spin self-energy (65) comes from the upper band  $E_{\mathbf{k}}$  of the dressed holon quasiparticle spectrum. During the above calculation, we find that the mode which opens downward and gives the incommensurate magnetic scattering at low energy is mainly determined by the first and second terms in the right side of the dressed spin self-energy (65), while the mode which opens upward and gives the incommensurate magnetic scattering at high energy is essentially dominated by the third and fourth terms in the right side of the dressed spin self-energy (65), then two modes meet at the commensurate  $[1/2, 1/2]$  resonance at intermediate energy. This means that within the framework of the kinetic energy driven superconductivity, as a result of self-consistent motion of the dressed holon pairs and spins, the incommensurate magnetic scattering at both low and high energies and commensurate resonance at intermediate energy are developed. This reflects that the low and high energy spin excitations drift away from the antiferromagnetic wave vector, or the zero point of  $W(\mathbf{k}_c, \omega)$  is shifted from  $[1/2, 1/2]$  to  $\mathbf{k}_c = \mathbf{k}_c^{(L)}$  at low energy and  $\mathbf{k}_c = \mathbf{k}_c^{(H)}$  at high energy. With increasing energy from low energy or decreasing energy from high energy, the spin excitations move towards to  $[1/2, 1/2]$ , i.e., the zero point of  $W(\mathbf{k}_c, \omega)$  in  $\mathbf{k}_c = \mathbf{k}_c^{(L)}$  at low energy or  $\mathbf{k}_c = \mathbf{k}_c^{(H)}$  at high

energy turns back to  $[1/2, 1/2]$ , then the commensurate  $[1/2, 1/2]$  resonance appears at intermediate energy. To show this point clearly, the function  $W(\mathbf{k}, \omega)$  in  $x_{\text{opt}} = 0.15$  for  $t/J = 2.5$  and  $t'/t = 0.3$  with  $T = 0.002J$  from (a)  $\mathbf{k}_1 = [(1 - \delta)/2, 1/2]$  via  $\mathbf{k}_2 = [1/2, 1/2]$  to  $\mathbf{k}_3 = [(1 + \delta)/2, 1/2]$  at  $\omega = 0.12J$  (solid line) and  $\omega = 0.4J$  (dashed line), and (b)  $\mathbf{k}_4 = [(1 - \delta')/2, (1 - \delta')/2]$  via  $\mathbf{k}_2 = [1/2, 1/2]$  to  $\mathbf{k}_5 = [(1 + \delta')/2, (1 + \delta')/2]$  at  $\omega = 0.4J$  (solid line) and  $\omega = 0.82J$  (dashed line) is plotted in Fig. 8, where there is a strong angular dependence with actual minima in  $[(1 - \delta)/2, 1/2]$  and  $[1/2, (1 - \delta)/2]$ ,  $[1/2, 1/2]$ , and  $[(1 - \delta')/2, (1 - \delta')/2]$  and  $[(1 + \delta')/2, (1 + \delta')/2]$  for low, intermediate, and high energies, respectively. These are exactly positions of the incommensurate magnetic scattering peaks at both low and high energies and commensurate resonance peak at intermediate energy determined by the dispersion of very well defined renormalized spin excitations. Since the essential physics is dominated by the dressed spin self-energy renormalization due to the dressed holon bubble in the dressed holon particle-particle channel, then in this sense the mobile dressed holon pairs (then the electron Cooper pairs) are the key factor leading to the incommensurate magnetic scattering peaks at both low and high energies and commensurate resonance peak at intermediate energy, i.e., the mechanism of the incommensurate magnetic scattering and commensurate resonance in the superconducting-state is most likely related to the motion of the dressed holon pairs (then the electron Cooper pairs). This is why the positions of the incommensurate magnetic scattering peaks and commensurate resonance peak in the superconducting-state can be determined in the present study within the  $t$ - $t'$ - $J$  model based on the kinetic energy driven superconducting mechanism, while the dressed spin energy dependence is ascribed purely to the self-energy effects which arise from the the dressed holon bubble in the dressed holon particle-particle channel.

## 1.4 The charge asymmetry in superconductivity of hole and electron doping

Superconductivity emerges when charge carriers, holes or electrons, are doped into the parent compound of cuprates [1, 50]. Both hole-doped and electron-doped cuprate superconductors have the layered structure of the square lattice of the  $\text{CuO}_2$  plane separated by insulating layers [5, 50]. It has been found from experiments that only an approximate symmetry in the phase diagram exists about the zero doping line between the electron and hole doping [51]. For the hole-doped case [1, 5], the antiferromagnetic long-

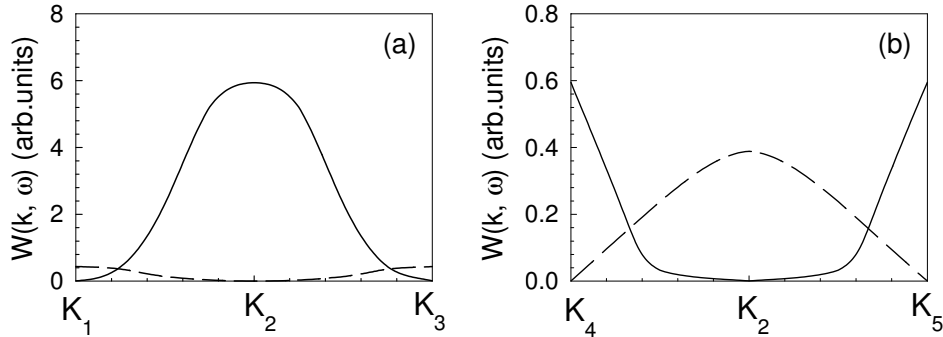


Figure 1.8: Function  $W(\mathbf{k}, \omega)$  in  $x_{\text{opt}} = 0.15$  for  $t/J = 2.5$  and  $t'/t = 0.3$  with  $T = 0.002J$  from (a)  $\mathbf{k}_1 = [(1 - \delta)/2, 1/2]$  via  $\mathbf{k}_2 = [1/2, 1/2]$  to  $\mathbf{k}_3 = [(1 + \delta)/2, 1/2]$  at  $\omega = 0.12J$  (solid line) and  $\omega = 0.4J$  (dashed line), and (b)  $\mathbf{k}_4 = [(1 - \delta')/2, (1 - \delta')/2]$  via  $\mathbf{k}_2 = [1/2, 1/2]$  to  $\mathbf{k}_5 = [(1 + \delta')/2, (1 + \delta')/2]$  at  $\omega = 0.4J$  (solid line) and  $\omega = 0.82J$  (dashed line).

range order disappears rapidly with doping, and is replaced by a disordered spin liquid phase, then the systems become superconducting over a wide range of the hole doping concentration, around the optimal  $x \sim 0.15$  [7]. However, the antiferromagnetic long-range order survives until superconductivity appears over a narrow range of the electron doping concentration around the optimal  $x \sim 0.15$  in the electron-doped case, where the maximum achievable superconducting transition temperature is much lower than that in the hole-doped case [50, 52, 53]. Although this electron-hole asymmetry is observed in the phase diagram [5, 51], the charge carrier Cooper pairs in both optimally electron- and hole-doped cuprate superconductors have a dominated d-wave symmetry [10, 39, 54, 55]. Since the strong electron correlation is common for both hole-doped and electron-doped cuprate superconductors, many of the physical properties of electron-doped cuprate superconductors resemble that of the hole-doped case. These show that both hole- and electron-doped cuprate superconductors have similar underlying superconducting mechanism. In this section, we study the charge asymmetry in superconductivity of hole- and electron-doped cuprate superconductors. We show that superconductivity appears over a narrow range of the electron doping concentration in the electron-doped case, and the maximum achievable superconducting transition temperature in the optimal doping is lower than that of the hole-doped case due to the electron-hole asymmetry.

For discussing the case of the electron doping, we can perform a particle-

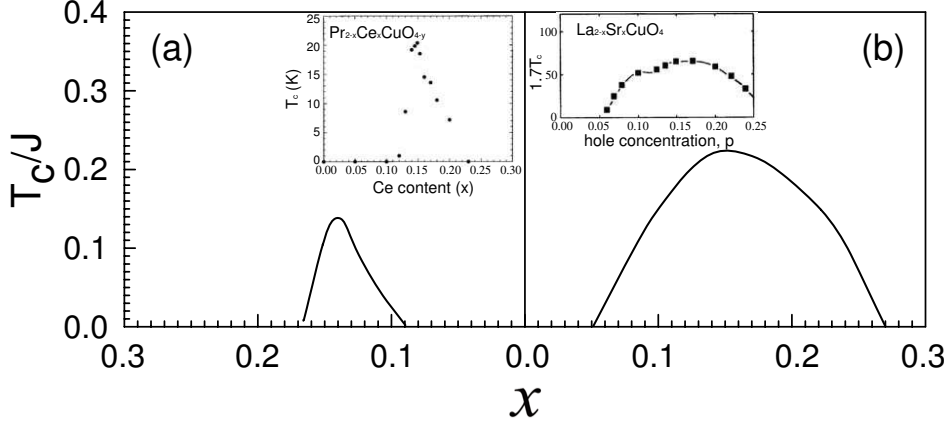


Figure 1.9: The superconducting transition temperature as a function of the doping concentration with (a)  $t/J = -2.5$  and  $t'/t = 0.3$  for the electron doping and (b)  $t/J = 2.5$  and  $t'/t = 0.3$  for the hole doping. Inset: the corresponding experimental results of  $\text{Pr}_{2-x}\text{Ce}_x\text{CuO}_{4-y}$  taken from Ref. [53] and  $\text{La}_{2-x}\text{Sr}_x\text{CuO}_4$  from Ref. [7]

hole transformation  $C_{i\sigma} \rightarrow C_{i-\sigma}^\dagger$  for the  $t$ - $t'$ - $J$  model (1), so that the difference between hole and electron doping is expressed as the sign difference of the hopping parameters [23], i.e.,  $t > 0$  and  $t' > 0$  for the hole doping and  $t < 0$  and  $t' < 0$  for the electron doping, then the  $t$ - $t'$ - $J$  model (1) in both hole- and electron-doped cases is always subject to an important on-site local constraint to avoid the double occupancy. Moreover, it has been shown that the absolute values of  $t$  and  $t'$  are almost same for both hole- and electron-doped cuprates [56]. In this case, we have followed the discussions in section 2 for the hole-doped case, and performed a calculation for the case of the electron doping. In Fig. 9(a), we plot the superconducting transition temperature in the case of the d-wave symmetry as a function of the electron doping concentration for  $t/J = -2.5$  and  $t'/t = 0.3$  in comparison with the corresponding experimental result of  $\text{Pr}_{2-x}\text{Ce}_x\text{CuO}_{4-y}$  [53] (inset). For comparison, the corresponding result of the hole doping in the case of the d-wave symmetry in Fig. 2 is also replotted in Fig. 9(b). Our results indicate that in analogy to the phase diagram of the hole-doped case, superconductivity appears over a narrow range of doping in the electron-doped side, where the superconducting transition temperature increases sharply with increasing doping in the underdoped regime, and reaches a maximum in the optimal doping  $x_{\text{opt}} \approx 0.14$ , then decreases sharply with increasing doping

in the overdoped regime. However, the maximum achievable superconducting transition temperature in the optimal doping in the electron-doped case is much lower than that of the hole-doped case due to the electron-hole asymmetry. Using a reasonably estimative value of  $J \sim 800\text{K}$  to  $1200\text{K}$  for the electron-doped cuprate superconductors, the superconducting transition temperature in the optimal doping is  $T_c \approx 0.136J \approx 108\text{K} \sim 163\text{K}$ , in semi-quantitative agreement with the corresponding experimental data [50, 53]. The essential physics of the doping dependent superconducting transition temperature in the electron-doped case is almost the same as in the hole-doped side, and detailed explanations have been given in section 2. On the other hand, it has been shown [56] that the antiferromagnetic long-range order can be stabilized by the  $t'$  term for the electron-doped case, which may lead to the charge carrier's localization over a broader range of doping, this is also why superconductivity appears over a narrow range of doping in electron-doped cuprate superconductors. Furthermore, we have discussed the spin response of the electron-doped cuprates in the superconducting-state, and the new feature of the spin response in the electron-doped cuprates in the superconducting-state is the energy dependence of the commensurate resonance peak at both low and intermediate energies and incommensurate magnetic scattering peaks at high energy. These and related theoretical results will be presented elsewhere.

## 1.5 Conclusion

Within the  $t$ - $t'$ - $J$  model, we have discussed the physical properties of doped cuprates in the superconducting-state based on the charge-spin separation fermion-spin theory. It is shown that the superconducting-state is controlled by both superconducting gap parameter and single particle coherence, and is the conventional Bardeen-Cooper-Schrieffer like, so that some of the basic Bardeen-Cooper-Schrieffer formalism [8] is still valid in quantitatively reproducing of the doping dependence of the superconducting gap parameter [40], the doping dependence of the superconducting transition temperature [7], and the electron spectral function in the superconducting-state [6, 22], although the superconducting Cooper pairing mechanism is driven by the kinetic energy by exchanging dressed spin excitations [20], and other exotic properties are beyond Bardeen-Cooper-Schrieffer theory. Although the symmetry of the superconducting-state is doping dependent, the superconducting-state has the d-wave symmetry in a wide range of doping. Within this d-wave superconducting-state, we have performed a systematic

calculation for the dynamical spin structure factor of doped cuprates in the superconducting-state in terms of the collective mode in the dressed holon particle-particle channel, and quantitatively reproduced all main features found in the inelastic neutron scattering experiments on cuprate superconductors, including the energy dependence of the incommensurate magnetic scattering at both low and high energies [15, 24, 25] and commensurate  $[\pi, \pi]$  resonance at intermediate energy [26, 27]. In particular, we have shown that the unusual incommensurate magnetic excitations at high energy have energies greater than the dressed holon pairing energy (then superconducting Cooper pairing energy), and are present at the superconducting transition temperature. Furthermore, we have studied the charge asymmetry of superconductivity in the hole and electron doping, and show that in analogy to the phase diagram of the hole-doped case, superconductivity appears over a narrow range of the electron doping concentration in the electron-doped side, and the maximum achievable superconducting transition temperature in the optimal doping in the electron-doped case is much lower than that of the hole-doped side due to the electron-hole asymmetry. Our present study also shows that the effect of the additional second neighbor hopping  $t'$  is to enhance the d-wave superconducting pairing correlation, and suppress the s-wave superconducting pairing correlation.

Within this framework of the kinetic energy driven superconductivity, we [57] have studied the electronic structure of cuprate superconductors. It is shown that the spectral weight of the electron spectrum in the antinodal point of the Brillouin zone decreases as the temperature is increased. With increasing the doping concentration, this spectral weight increases, while the position of the sharp superconducting quasiparticle peak moves to the Fermi energy. In analogy to the normal-state case, the superconducting quasiparticles around the antinodal point disperse very weakly with momentum. Our results also show that the striking behavior of the superconducting coherence of the quasiparticle peaks is intriguingly related to the strong coupling between the superconducting quasiparticles and collective magnetic excitations.

### Acknowledgements

The author would like to thank Dr. Huaiming Guo, Dr. Yu Lan, Dr. Yiny Liang, Dr. Bin Liu, and Professor Y.J. Wang for the helpful discussions. This work was supported by the National Natural Science Foundation of China under Grant Nos. 10125415 and 90403005, and the Grant from Beijing Normal University.



# Bibliography

- [1] Bednorz J.G. and Müller K.A. *Z. Phys.* **B64**, 189 (1986).
- [2] Anderson P.W. *Science* **235**, 1196 (1987).
- [3] Anderson P.W. *Phys. Rev. Lett.* **67**, 2092 (1991); *Science* **288**, 480 (2000); *Physica* **C341-348**, 9 (2000); cond-mat/0108522.
- [4] Laughlin R.B. *Phys. Rev. Lett.* **79**, 1726 (1997); *J. Low. Tem. Phys.* **99**, 443 (1995).
- [5] See, e.g., Kastner M.A.; Birgeneau R.J.; Shiran G. and Endoh Y. *Rev. Mod. Phys.* **70**, 897 (1998).
- [6] Ding H.; Engelbrecht J.R.; Wang Z.; Campuzano J.C.; Wang S.C.; Yang H.B.; Rogan R.; Takahashi T.; Kadowaki K. and Hinks D.G. *Phys. Rev. Lett.* **87**, 227001 (2001); He R.H.; Feng D.L.; Eisaki H.; Shimoyama J.-I.; Kishio K. and Gu G.D. *Phys. Rev.* **B69**, 220502 (2004).
- [7] See, e.g., Tallon J.L.; Loram J.W.; Cooper J.R.; Panagopoulos C. and Bernhard C. *Phys. Rev.* **B68**, 180501 (2003).
- [8] Bardeen J.; Cooper L.N. and Schrieffer J.R.; *Phys. Rev.* **108**, 1175 (1957); Schrieffer J.R. *Theory of Superconductivity*, Benjamin, New York, 1964.
- [9] Chester G. *Phys. Rev.* **103**, 1693 (1965).
- [10] See, e.g., Tsuei C.C. and Kirtley J.R. *Rev. Mod. Phys.* **72**, 969 (2000).
- [11] Yeh N.-C.; Chen C.T.; Hammerl G.; Mannhart J.; Schmehl A.; Schneider C.W.; Schulz R.R.; Tajima S.; Yoshida K.; Garrigus D. and Strasik M. *Phys. Rev. Lett.* **87**, 087003 (2001); Deutscher G. *Nature* **397**, 410 (1999).

- [12] Yamada K.; Lee C.H.; Kurahashi K.; Wada J.; Wakimoto S.; Ueki S.; Kimura H.; Endoh Y.; Hosoya S. and Shirane G. *Phys. Rev.* **B57**, 6165 (1998).
- [13] Dai P.; Mook H.A.; Hunt R.D. and Doğan F. *Phys. Rev.* **B63**, 54525 (2001); He H.; Bourges P.; Sidis Y.; Ulrich C.; Regnault L.P.; Pailhès S.; Berzigiarova N.S.; Kolesnikov N.N. and Keimer B. *Science* **295**, 1045 (2002); Christensen N.B.; McMorrow D.F.; Rønnow H.M.; Lake B.; Hayden S.M.; Aeppli G.; Perring T.G.; Mangkorntong M.; Nohara N. and Tagaki H. *Phys. Rev. Lett.* **93**, 147002 (2004).
- [14] Wakimoto S.; Zhang H.; Yamada K.; Swainson I.; Kim H. and Birgeneau R.J. *Phys. Rev. Lett.* **92**, 217004 (2004); Fujita M.; Yamada K.; Hiraka H.; Gehring P.M.; Lee S.H.; Wakimoto S. and Shirane G. *Phys. Rev.* **B65**, 064505 (2002); Wakimoto S.; Shirane G.; Endoh Y.; Hirota K.; Ueki S.; Lee Y.S.; Gehring P.M. and Lee S.H. *Phys. Rev.* **B60**, R769 (1999).
- [15] Hayden S.M.; Mook H.A.; Dai P.; Perring T.G. and Doğan F. *Science* **429**, 531 (2004); Stock C.; Buyers W.J.; Cowley R.A.; Clegg P.S.; Coldea R.; Frost C.D.; Liang R.; Peets D.; Bonn D.; Hardy W.N. and Birgeneau R.J. *Phys. Rev.* **B71**, 024522 (2005).
- [16] See, e.g., Dagotto E. *Rev. Mod. Phys.* **66**, 763 (1994).
- [17] Capone M.; Fabrizio M.; Castellani C. and Tosatti T. *Science* **296**, 2364 (2002).
- [18] Molegraaf H.J.A.; Pressure C.; van der Marel D.; Kes P.H. and Li M. *Science* **295**, 2239 (2002).
- [19] Feng Shiping; Qin Jihong and Ma Tianxing *J. Phys. Condens. Matter* **16**, 343 (2004); Feng Shiping; Ma Tianxing and Qin Jihong *Mod. Phys. Lett.* **B17**, 361 (2003); Feng Shiping; Su Z.B. and Yu L. *Phys. Rev.* **B49**, 2368 (1994).
- [20] Feng Shiping *Phys. Rev.* **B68**, 184501 (2003).
- [21] Ma Tianxing; Guo Huaiming and Feng Shiping *Mod. Phys. Lett.* **B18**, 895 (2004); Feng Shiping; Ma Tianxing and Guo Huaiming *Physica C* **436**, 14 (2006).

- [22] Well B.O.; Shen Z.-X.; Matsuura A.; King D.M.; Kastner M.A.; Greven M. and Birgeneau R.J. Phys. Rev. Lett. **74**, 964 (1995); King C.; White P.J.; Shen Z.-X.; Tohyama T.; Shibata Y.; Maekawa S.; Wells B.O.; King Y.J.; Birgeneau R.J. and Kastner M.A. Phys. Rev. Lett. **80**, 4245 (1998).
- [23] Ma Tianxing; Guo Huaiming and Feng Shiping Phys. Lett. **A337**, 61 (2005); Liu Bin; Liang Ying; Feng Shiping and Chen Wei Yeu Phys. Rev. **B69**, 224506 (2004).
- [24] Arai M.; Nishijima T.; Endoh Y.; Egami T.; Tajima S.; Tomimoto K.; Shiohara Y.; Takahashi M.; Garret A. and Bennington S.M. Phys. Rev. Lett. **83**, 608 (1999).
- [25] Tranquada J.M.; Woo H.; Perring T.G.; Goka H.; Gu G.D.; Xu G.; Fujita M. and Yamada K. Nature **429**, 534 (2004).
- [26] Bourges P.; Keimer B.; Pailh es S.; Regnault L.P.; Sidis Y. and Ulrich C. Physica C **424**, 45 (2005); He H.; Sidis Y.; Bourges P.; Gu G.D.; Ivanov A.; Koshizuka N.; Liang B.; Lin C.T.; Regnault L.P.; Schoenherr E. and Keimer B. Phys. Rev. Lett. **86**, 1610 (2001).
- [27] Bourges P.; Sidis Y.; Fong H.F.; Regnault L.P.; Bossy J.; Ivanov A. and Keimer B. Science **288**, 1234 (2000).
- [28] Nazarenko A.; Vos K.J.E.; Haas S. and Dagotto E. Phys. Rev. **B51**, 8676 (1995); Belinicher V.I.; Chernyshev A.L. and Shubin V.A. Phys. Rev. **B54**, 14914 (1996).
- [29] Martins G.B.; Eder R. and Dagotto E. Phys. Rev. **B60**, R3716 (1999); Martins G.B.; Xavier J.C.; Gazza C.; Vojta M. and Dagotto E. Phys. Rev. **B63**, 014414 (2000); Martins G.B.; Gazza C.; Xavier J.C.; Feiguin A. and Dagotto E. Phys. Rev. Lett. **84**, 5844 (2000).
- [30] Shen Z.X.; Dessau D.S.; Wells B.O.; King D.M.; Spicer W.E.; Arko A.J.; Marshall D.; Lombardo L.W.; Kapitulnik A.; Dickinson P.; Do-niach S.; DiCarlo J.; Loeser T. and Park C.H. Phys. Rev. Lett. **70**, 1553 (1993); Ding H.; Norman M.R.; Campuzano J.C.; Randeria M.; Bellman A.F.; Yokoya T.; Takahashi T.; Mochiku T. and Kadowaki K. Phys. Rev. **B54**, R9678 (1996).
- [31] Bozovic I.; Logvenov G.; Verhoeven M.A.; Gaputo P.; Goldobin E. and Geballe T.H. Nature **422**, 873 (2003).

- [32] See, e.g., Tyablikov S.V. *Method in the Quantum Theory of Magnetism*, Plenum, New York, 1967.
- [33] Feng Shiping and Song Yun *Phys. Rev.* **B55**, 642 (1997); Yuan Feng and Feng Shiping *Phys. Lett.* **A271**, 429 (2000).
- [34] Kondo J. and Yamaji K. *Prog. Theor. Phys.* **47**, 807 (1972).
- [35] Eliashberg G.M. *Sov. Phys. JETP* **11**, 696 (1960); Scalapino D.J.; Schrieffer J.R. and Wilkins J.W. *Phys. Rev.* **148**, 263 (1966).
- [36] Zubarev D.N. *Sov. Phys. Usp.* **3**, 201 (1960).
- [37] Feng Shiping and Huang Zhongbing, *Phys. Lett.* **A232**, 293 (1997); Yuan Feng; Qin Jihong; Feng Shiping and Chen W.Y. *Phys. Rev.* **B67**, 134505 (2003).
- [38] Chaudhari P. and Lin S.Y. *Phys. Rev. Lett.* **72**, 1084 (1994); Wu D.H.; Mao J.; Mao S.N.; Peng J.L.; Xi X.X.; Venkatesan T.; Greene R.L. and Anlage S.M. *Phys. Rev. Lett.* **70**, 85 (1993); Anlage S.M.; Langley B.W.; Deutscher G.; Halbritter J. and Beasley M.R. *Phys. Rev.* **B44**, 9764 (1991).
- [39] Martindale J.A.; Barrett S.E.; ÓHara K.E.; Slichter C.P.; Lee W.C. and Ginsberg D.M. *Phys. Rev.* **B47**, 9155 (1993); Hardy W.N.; Bonn D.A.; Morgan D.C.; Liang R. and Zhang K. *Phys. Rev. Lett.* **70**, 3999 (1994); Wollman D.A.; Van Harlingen D.J.; Lee W.C.; Ginsberg D.M. and Leggett A.J. *Phys. Rev. Lett.* **71**, 2134 (1993).
- [40] Wen H.H.; Yang H.P.; Li S.L.; Zeng X.H.; Soukiassian A.A.; Si W.D. and Xi X.X. *Europhys. Lett.* **64**, 790 (2003).
- [41] Biswas A.; Fournier P.; Qazilbash M.M.; Smolyaninova V.N.; Balci H. and Greene R.L. *Phys. Rev. Lett.* **88**, 207004 (20024).
- [42] Tsuei C.C.; Kirtley J.R.; Hammerl G.; Mannhart J.; Raffy H. and Li Z.Z. *Phys. Rev. Lett.* **93**, 187004 (2004).
- [43] Uemura Y.J.; Luke G.M.; Sternlieb B.J.; Brewer J.H.; Carolan J.F.; Hardy W.N.; Kadono R.; Kempton J.R.; Kiefl R.F.; Kretzmann S.R.; Mulhern P.; Riseman T.M.; Williams D.L.; Yang B.X.; Uchida S.; Takagi H.; Gopalakrishnan J.; Sleigh A.W.; Subramanian M.A.; Chien C.L.; Cieplak M.Z.; Xiao G.; Lee V.Y.; Statt B.W.; Stronach C.E.;

- Kossler W.J. and Yu X.H. Phys. Rev. Lett. **62**, 2317 (1989); Uemura Y.J.; Le L.P.; Luke G.M.; Sternlieb B.J.; Wu W.D.; Brewer J.H.; Riseman T.M.; Seaman C.L.; Maple M.B.; Ishikawa M.; Hinks D.G.; Jorgensen J.D.; Saito G. and Yamochi H. Phys. Rev. Lett. **66**, 2665 (1991).
- [44] Shamoto S.; Sato M.; Tranquada J.M.; Sternlib B.J. and Shirane G. Phys. Rev. **B48**, 13817 (1993).
- [45] See, e.g., Shen Z.X. and Dessau D.S. Phys. Rep. **70**, 253 (1995); Damascelli A.; Hussain Z. and Shen Z.X. Rev. Mod. Phys. **75**, 475 (2003).
- [46] Matsui H.; Sato T.; Takahashi T.; Wang S.C.; Yang H.B.; Ding H.; Fujii T.; Watanabe T. and Matsuda A. Phys. Rev. Lett. **90**, 217002 (2003).
- [47] DeWilde Y.; Miyakawa N.; Guptasarma P.; Iavarone M.; Ozyuzer L.; Zasadzinski J.F.; Romano P.; Hinks D.G.; Kendziora C.; Crabtree G.W. and Gray K.E. Phys. Rev. Lett. **80**, 153 (1998).
- [48] Hinkov V.; Pailh es S.; Bourges P.; Sidis Y.; Ivanov A.; Kulakov A.; Lin C.T.; Chen D.P.; Bernhard C. and Keimer B. Science **430**, 650 (2004).
- [49] Feng Shiping and Huang Zhongbing Phys. Rev. **B57**, 10328 (1998); Yuan Feng; Feng Shiping; Su Z.B. and Yu L. Phys. Rev. **B64**, 224505 (2001); Feng Shiping; Yuan Feng; Su Z.B. and Yu L. Phys. Rev. **B66**, 064503 (2002).
- [50] Tokura Y.; Takagi H. and Uchida S. Nature **337**, 345 (1989).
- [51] Sawa A.; Kawasaki M.; Takagi H. and Tokura Y. Phys. Rev. **B66**, 014531 (2002).
- [52] Takagi H.; Uchida S. and Tokura Y. Phys. Rev. Lett. **62**, 1197 (1989).
- [53] Peng J.L.; Maiser E.; Venkatesan T.; Greene R.L. and Czjzek G. Phys. Rev. **B55**, R6145 (1997).
- [54] Armitage N.P.; Lu D.H.; Feng D.L.; Kim C.; Damascelli A.; Shen K.M.; Ronning F.; Shen Z.-X.; Onose Y.; Taguchi Y. and Tokura Y. Phys. Rev. Lett. **86**, 1126 (2001).

- [55] Tsuei C.C. and Kirtley J.R. Phys. Rev. Lett. **85**, 182 (2000).
- [56] Hybertson M.S.; Stechel E.; Schuter M. and Jennison D. Phys. Rev. **B41**, 11068 (1990).
- [57] Guo Huaiming and Feng Shiping Phys. Lett. **A361**, 382 (2007);  
Feng Shiping and Ma Tianxing Phys. Lett. **A350**, 138 (2006); Guo  
Huaiming and Feng Shiping Phys. Lett. **A355**, 473 (2006).